SCIENTIFIC CULTURE
www.sci-cult.com

SCIENTIFIC CULTURE, Vol. 11, No. 1, (2025), pp. 1-24
Open Access. Online & Print

DOI: 10.5281/zenodo.14369342

INVESTIGATION OF THE POWER LAW DEPENDENCE OF OBSIDIAN DIFFUSION TEMPERATURE WITH HYDRATION THICKNESS AND ITS OBSIDIAN HYDRATION DATING IMPLICATIONS: Part II

Liritzis Ioannis[1,2] and Andronache Ion[1]

[1]Alma Mater Europaea University (AMEU) Slovenska Ulica 17, 2000, Maribor, Slovenia
[2]European Academy of Sciences & Arts, St. Peter-Bezirk 10, A-5020 Salzburg, Austria

Received: 25/11/2024
Accepted: 10/12/2024

Corresponding author: I. Liritzis
(ioannis.liritzis@almamater.si; ioannis.liritzis@euro-acad.eu)

ABSTRACT

Obsidian hydration dating (OHD) has been a concern of research into chronological issues of ancient obsidian artifacts. The OHD is based on the power law equation relating to hydration depth (measured microscopically or by SIMS), hydration rate and time.

Experimental aged data at high temperature (ca 140 – 180 ^{o}C) from five geographically world dispersed obsidian sources (California, Mexico, Peru, New Zealand) and at low temperature (10-40^{o}C) (New Guinea) are used to explore the functional dependence of obsidian diffusion temperature with hydration thickness and pixels.

A consistent power law dependent model for hydration rim/year and pixels/year versus temperature has been revealed for the first time, extending earlier indication with fewer data. Combination in tandem of data of high T and low aged data as well as reconstructed low T data, are used. The exponents lie on average between 3.2 and 5.5; the coefficients of the equations exhibit uniformity; all sources with Umleang except NZ and the high T of NZ have E-11, all high T with Wekwok of the order of E-07.

Use of this model has been provisionally applied to reported ages of archaeological obsidian blades from Easter Island, Napa Valley California, Japan, Ethiopia, Papua New Guinea and the first available results hint at a novel approach to OHD. Advantages and limitations are discussed.

KEYWORDS: Diffusion, Temperature, Hydration, Pixels, Archaeological, Rim, SIMS, New Zealand, Umleang, Wekwok, Peru, Mexico, California, Napa Valley, Bodie Hill, Papua, Easter Island, Japan, Ethiopia.

1. INTRODUCTION

The mechanism of diffused water through the surface of archaeological Obsidian blades, a mainly temperature-dependent and concentration-driven phenomenon, related to the obsidian hydration dating (OHD), is a subject of ongoing development.

Diffusion is an essential transport in many rock and biological systems and is known to be susceptible to environmental and intrinsic structure and inhomogeneity. The most basic definition of diffusion is that it presumes a homogeneous environment with a continuously increasing mean squared displacement and a Gaussian distribution of particle displacements.

The functional power law has been observed in several cases. For example, in metallic glasses when under compression, the volume (V) of a Metallic Glasses change precisely to the 2.5 power of its principal diffraction peak position (Ma et al., 2009; Zeng 2016). Also, in the physical-chemical properties rocks the Terahertz (THz) time domain spectroscopy (TDS, where THz TDS) is used to measure THz optical properties, i.e., refractive indices and absorption coefficients of borosilicate, tellurite, and chalcogenide glass families. It was observed that the THz optical properties depend on glass compositions and fitting parameters for the power law model used to describe these properties and show how it can be universally applied to several glass families (Tostanoski & Sundaram, 2023). In rheological properties of minerals and rocks power law of exponent 3-5 has been reported (Karato, 2013), and in biological systems (Novikov et al., 2014).

These different approaches lead to similar forms suggesting that power laws, and particularly the values of power law exponents, capture a fundamental property of the observed dynamics. It has been proposed that the value of power law exponents defines universality classes capturing the dimensionality and type of disorder present in the diffusion environment (Lee et al., 2020).

For water to penetrate obsidian, a water molecule must have enough energy to stretch the glass matrix and enter one of the spaces in between. This energy is directly related to the temperature in Kelvins, which means that the rate of hydration is dependent on temperature.

Having made the recent investigation of fractals (Liritzis et al., 2023) on the variations of water and structural entities within the obsidian in the micron and nanoscale of divided hydration and pure obsidian, the present work focused on the growth rate of water in various controlled temperatures and on archaeological hydrated artifacts. Making use of the obtained rates tentative dates for five relatively known age obsidian artifacts are made.

The ongoing interest in OHD is revived recently (Nakazawa, et al. 2023; Laskaris and Liritzis, 2020; Liritzis & Laskaris, 2021; Stevenson, et al., 2019a; 2023).

Sixty-six years ago, the dating of obsidian stone tools from the last time they were used by prehistoric people had been proposed, observing that a newly exposed surface of obsidian takes on water from the environment at a known rate that can be used to calculate the time elapsed since exposure (Friedman and Smith, 1960). Following that, the hydration technique was further investigated, and several variations of the so-called obsidian hydration dating (OHD) method were reported, proposing both empirical and intrinsic rate methods. Secondary ion mass spectroscopy (SIMS) has been used over the last 20 years to properly quantify the hydration profile (water content using H^+ versus depth) in a phenomenology manner, and Fourier Transform Infrared (FTIR) spectroscopy to monitor the absorbed diffused water peaks (Stevenson and Novak, 2011; Liritzis and Laskaris, 2011, 2012; Laskaris and Liritzis, 2020; Liritzis and Laskaris, 2021). Models explaining the diffusion process are used to determine the age by modeling the hydration profile (Liritzis and Laskaris, 2021; Stevenson et al., 2021a).

After the launch of the empirical OHD approach, the precise mechanism by which water diffusion takes place in amorphous rhyolitic glass such as obsidian is still under investigation (Doremus, 1969; Crank, 1976; Zhang et al., 1991; Zhang and Behrens, 2000; Doremus, 2000, 2002; Anovitz et al., 2006; Laskaris and Liritzis, 2020).

Water diffusion is a complicated and dynamic process at the start of the diffusion process, as evidenced by laboratory accelerating hydration tests (Stevenson and Novak, 2011; Anovitz et al., 2004)

Based upon Fick's law of diffusion, the water diffusion is a concentration driven process and depends on environmental temperature (higher temperature longer hydration rims) (Crank 1976).

As a result of diffusion, hydration has a high surface concentration while the diffusion coefficient decreases (Liritzis 2014). Following up on Liritzis' technique (Liritzis and Diakostamatiou, 2002; Liritzis et al., 2004; Liritzis, 2006, 2014) it has been proposed that this change may be due to glass surface relaxation when tension in the near-surface region is released (Webb, 2021).

The water from the burial site is absorbed by the obsidian's surface, resulting in the production of a hydration rim at its interface layer (a few microns under the surface). The hydration of obsidians is a complex, diffusion-based phenomenon that is greatly influenced by temperature, the intrinsic (structural) water

of the artifact, water concentration on the glass surface and the glass stoichiometric structure, but also relative humidity (R_H) (Mazer et al., 1991; Anovitz et al., 2006).

The variable temperature of the burial environment and various factors participating in the diffusion process during the tool's lifetime contribute to the final shape of the diffusion profile (concentration vs depth), the SIMS sigmoid curve.

For dating purposes, Friedman and Smith (1963) suggested the empirical power law equation (eq. 1):

$$x^2=k*t \quad (1)$$

Where x is the thickness of the hydration rim in microns (μm) [abbr. to um], t is the age in years, k is the hydration rate at a particular temperature/relative humidity (Liritzis 2014; Friedman and Smith 1960; Rogers, 2007, 2008b; Rogers and Duke, 2011; Liritzis 2014).

Eq.2 is essentially the hydration rate k (μm^2/day) of Arrhenius as in eq. 2:

$$k=A*e^{-E/RT} \quad (2)$$

T is the absolute temperature (Kelvin) which represents the effective hydration temperature (EHT), k is the diffusion coefficient (μm^2/day), A is a pre-exponential replacement, as a source-specific constant, E the activation energy (joules per mole) again as a source or burial environment's constant and R the gas constant (8.314 J / mol·K joules per degree per mole). The *k* is calculated from high temperature aged experiments and is then used in eq.1.

The Arrhenius equation can be rearranged for example, taking the logarithm of both sides yields the equation above in the linear form.

$$k=A*e^{-E/RT} \rightarrow \ln k=-(E/RT)+\ln A \quad (3)$$

Then, in the plot of Lnk vs. 1/T, the intercept is the LnA, the slope is –(E/RT) and all variables can be found (in fact the slope appears as - (- E/R)=E/R.

The primary issue in all techniques is determining the "effective temperature" T (EHT), which determines the diffusion rate (Smith et al., 2003). This is the temperature required to produce equivalent hydration rim as the fluctuating temperature over the identical archaeological duration. EHT can never be lower than the mean temperature, as per the Arrhenius equation's mathematical structure. The average temperature experienced by the artifact during its interment period is known as the burial period's mean temperature (Rogers 2007, 2008 a, b, 2012). Another issue concerns the extrapolation of high temperature aged data to environmental temperatures.

We are also concerned about the similarities in water diffusion rates between the controlled experimental temperature range in laboratory settings (90 to 190 °C) and the natural environmental temperature range (0 to 40 °C). Investigating glass hydration above and below the glass transition temperature (about 400°C). Anovitz et al., (2008) found clear variations in the mechanisms underlying water diffusion. Water molecules can permeate the softer glass at higher temperatures, causing the glass to rapidly expand in volume to make room for the new material. This promotes diffusion, which quickly interconverts molecules of H2Om and OH and becomes essentially independent of the composition of the glass. (W is total water in wt.% for range of structural water values used in this fit of 0.1 < W < 1.02 wt.%, the w is total Water %H2Ot. In the present investigation we use obsidians with H2Ot less than 0.2% so all the water is %OH, thus there is no structural H2O in these obsidian specimens, Ambrose et al., 2004b).

At lower temperatures, on the other hand, the situation is very different. A stress or hydration layer forms because of the obsidian's inability to sufficiently adapt to the volume increase brought on by the incoming water. Molecular water is the main species introduced, and the conversion to OH is impeded. Notably, their experimental findings showed that, for example for the Pachuca obsidian, diffusion coefficients and temperature had a distinct linear connection between 30 and 150 °C (Anovitz et al., 2008, Fig. 3). This result supports the study hypothesis of Stevenson and Novak (2011), which states that the kinetics of hydration are constant at temperatures between 190 °C and room temperature. However, more evidence and data are needed to postulate earlier ascertainment.

The estimation of hydration rates in archaeological samples has been achieved through field studies connecting cultural artifacts to contexts of known age determined by an independent dating method. The most used method links hydration levels with thickness and radiocarbon ages.

The measured obsidian samples are strictly stratigraphically connected context-wise, but no calibration was achieved at first when the relationship between the 14C dates and the hydration depth was investigated. Using this relationship, Rogers and Stevenson (2023a) calculated the hydration rates via obsidian-radiocarbon association. The accuracy of the scientifically based model, depending on the obsidian source, ranges from 5% to 13%. Since the authors conclude that there is no guarantee that the ad hoc best-fit equation will be accurate beyond the data set on which it is based, the process was not advised even though it is conceivable to develop one from archeological data for a particular investigation.

Today the main methodological approaches used in OHD have been summarized elsewhere (Liritzis et al., 2024a).

Rogers (2007) computed an effective hydration temperature from a numerical integration of the hydration rate over the temperature model determining an EHT for each artifact, based on site elevation and burial depth, and applied a rim correction factor to correct the rim value to a consistent reference temperature. Furthermore, work on Bodie Hills obsidian concludes it would be imprudent to assume an accuracy greater than roughly 20% in doing chronometric studies (Rogers 2008 a,b).

At any rate, the effect of temperature on the hydration rate is significant and the result of the hydration layer expressed in terms of pixels and fractals is still an ongoing development; see on rates Rogers and Duke (2011), Rogers (2011) and on fractals Liritzis et al., (2024b).

We are aware of the limitations and the errors involved in a) the recording of rim thickness / define the boundary at the hydration tail, b) the different scales in thin sectioned images have problems of standardization of thickness to pixels ratio, and c) execution of unconstrained aged diffusion experiments. But it is challenging to develop an independent dating method, in addition to luminescence and radiocarbon, with applications ranging from about 200 BP to around 1,000,000 BP.

The present work is a follow up of an earlier (Liritzis et al., 2024a, Part I) and explores the power law functional temperature dependence of the hydration in obsidians, of hydration thickness in μm, and pixels of the hydration area in relation to: i) the different sources of obsidian for high and low experimentally aged data, ii) the role of the variable pristine water content, iii) power law for five obsidian sources, and v) use the power law to date archaeological obsidian blades from Easter island, Japan and New Guinea, Napa Valley and Ethiopia.

Compared to the classical Arrhenius approach (i, ii above) the present investigation is an alternative approach for a functional behavior on temperature in the diffusion process. It is theoretically and experimentally supported and interesting results are obtained. It advances the field treating the obsidian from a global perspective.

2. MATERIALS, METHODS AND DATA

2.1 The five geological sources

Obsidian from five (5) geological sources were used for the high temperature and two (2) for the low T aged experiments in this analysis. These includes two locations (SA4D, 13J) within the Bodie Hills volcanic field, and single samples from Chivay (CPQ009F), Peru; Hahei, New Zealand, and Ucareo (UC-16A), Mexico. The low temperature aged obsidians are from New Guinea (Umleang and Wekwok) (abbreviations of sources throughout the text with their initials).

The Bodie Hills (BH) are a mountain range located along the California-Nevada border. The Bodie Hills Volcanic Field (BHVF) is composed of approximately twenty major eruptive centers encompassing more than 700 square kilometers (John et al., 2015). The volcanic field is known for its geologic complexity (John et al., 2012). The obsidian surface deposits occur as discrete terrace outcrops of cobble or as alluvially deposited lag flows. The extent of the Bodie Hills Obsidian Quarry (CA-MNO-4527) has been surveyed over the last twenty years with nearly 1618 hectares of deposit being defined (Halford 2008). The infrared structural water analysis of 114 samples from Bodie Hills revealed there to be obsidian source areas that varied spatially in their hydroxyl content and ranged between 0.10-0.25%OH. (Rogers and Stevenson 2023b; Stevenson et al., 2021b, 2024c).

We know less about the water content variability for the remaining sources. The Hahei geological source is in North Island, New Zealand (NZ), and it is one of many deposits in the Coromandel Peninsula that were exploited by the indigenous Maori population (Moore 2011, 2013). A geological hand sample was provided by the University of Auckland. Samples from Chivay and Ucareo were provided by the University of Missouri Archaeometry Laboratory. The Chivay source in the southern highlands of Peru has been documented by Glascock et al. (2007) and the Ucareo source chemically characterized by Glascock (2002) is from central Mexico. The water contents from these single hand samples were determined using standard analytical procedures on polished thick sections (von Aulock 2014; Stevenson et al. 2019). The structural water contents for all samples are given where available in **APPENDIX Table A1.**

Obsidian hydration rates were developed for each geological source. Five 1 x 1 cm coupons were cut from each flake for accelerated hydration. The experiment consisted of sample hydration at five reaction temperatures between 140°C and 180°C at ten-degree intervals. The reaction cannisters consisted of stainless-steel vessels with an interior volume of 23ml. One sample was placed within each vessel on a wire mesh support in the center of the compartment and 0.2g of distilled water was added. This maintained the cannister environment at 100% relative humidity during the reaction period. There was no contact between the small amount of water at the base of the cannister and the sample.

The cannisters were sealed and placed in Thermo mechanical convection ovens at 140-180°C and hydrated 30-81 days. At the end of this period the canisters were removed from the oven and quenched un-

der tap water. Petrographic thin sections were prepared on the Bodie Hills samples by Willamette Analytics and the hydration layer widths were measured at 600x using ImageJ pixel imaging. Origer and Associates measured the hydration layers on the Chivay, Hahei, and Ucareo samples using a filar screw eyepiece.

The low temperature aged obsidians are from New Guinea: the Umleang hydrated at 10°C-40oC for 9569 days (26.2 years) (Stevenson et al., 2002) and from Wekwok, hydrated at 10-40oC for 11.6-15.2 years, both have a water content of about 0.10%OH (Ambrose and Novak, 2012; Ambrose et al., 2004b) (**APPENDIX Table A1**).

The archaeological mostly well dated samples come from a) Easter Island site 10-241 Maunga Tari obsidian and C14 with an average rim 1.5um (ranges from 1.41 to 2.41um) a burial temperature of 21.9-22.2°C, measured by the logs buried for one year at different depths. The age range of the site is 550-1100 years BP; the OHD of seventeen blades varies between 520-900 years BP, and the cal. C-14 vary between 400-600 years BP, with an average of 1.5um of ca. 600 years BP (Stevenson 1993; 2024 personal communication); b) another archaeological blades derive from Papua New Guinea, Manus island Pamwak site, spanning to a depth of around 150 cm and cal. C-14 ages range from to 5th to 14th millennia BP (includes late glacial) (Ambrose 1994). The site (2° south of the equator) is archaeologically important because of the richness of the remains both faunally and artefactually, but particularly for the time range of its occupation based on radiocarbon dates extending to around 14,000 BP from about midway through the 3.8 m depth of the site. Temperature regime recorded from the main Manus Island at 27.2°C±2.8 (McAlpine et al., 1983), and measured at the site over a 3-week period as 25°C.

At 60cm depth the C14: 7732±89 BP. With a mean hydration thickness of 10.49±0.49 um. At any rate the average T°C is not measured well and hence based on C-14 result we accept temp as being 23-24°C at 60cm depth.

For another age of Papua of 11.82 um the cal. C-14 BP 10883-10365 at 95cm depth. Last for sample at 125cm depth corresponds to 14000 cal C-14 years BP from the linear extrapolation curve of depth versus age.

C) two from Japan one at Ocharasenai site, rim=2.73±0.511 um, age 4451-5105 BP and by C-14 age of context is 4597 ± 30 cal. BP, T=6.8-6.9 °C annual surface or 7.94°C EHT., and the other was Kyo-Shirataki 3 (Hokkaido), rim=4.5 um, EHT= 8-9°C/9-11°C reported, 17-19,000 yrs cal. BP (Nakazawa, 2016).

D) Three obsidians from Napa Valley (NV) in northern California: NV-1.9, NV-2.8, NV-4.5, NV-5.9, and NV-7.7 (NV stands for Napa Valley and the number of hydration layers in microns).

E) One Ethiopian blade PE-21 coming from a cave in Africa of the Middle Stone Age Ethiopian rock shelter of Porc Epic Dire Dawa which is supposed to date to approximately 60-70kya. Estimating the temperature in caves in Ethiopia are 22-24°C range (Clark et al., 1984; Fernandez et al., 2007). The sample is problematic in their dating (aged experiments were not hydrated properly and Late Stone Age (LSA) and lingering Middle Stone Age (MSA) artifacts were naturally mixed (Singer & Wymer, 1982).

2.2 Methodology

RGB images with obsidians were converted to grayscale. After images were segmented (extract only rim) and binarized (black pixels = obsidian without rim and white pixels = rim). Using ImageJ, we measured the number of white pixels corresponding to the rim[1].

Power law: Power law represents a mathematical relationship where a change in one quantity is proportional to a power of the change in another quantity, regardless of their initial values. This means that one quantity varies as a power of the other, and the exponent in the power law equation determines the nature of this relationship. We used power trendline from Microsoft Excel. A power trendline is a curved line that is particularly suitable for data sets where measurements increase at a consistent rate.

The formula of power law is:

$$y = ax^b \quad (4)$$

"y" represents the dependent variable, (pixels/yr or microns /yr (vertical axis). The simple growth rate of depth/time (um/year) is used for the alternative rate k of eq.1 (um²/time), as both change proportionally to the growth rate at least for environmental T of 10-30°C (see **APPENDIX Fig.A3**).

"x" represents the independent variable, Temperature (horizontal axis).

"a" is the coefficient.

"b" is the exponent or power.

The values of "a" and "b" are determined by Excel based on the data points to provide the best fit for the power trendline. One can use this formula to make

[1] Counting Pixels: ImageJ processes the image as a grid of pixels. Using the Analyze > Histogram or Analyze > Measure functions, ImageJ counts the number of pixels for each intensity value. For a binary image, the total number of white pixels (rim) is determined by the count of pixels with a value of 255.

predictions or analyze the relationship between data variables.

3. RESULTS

The experimental data of hydration rim developed under laboratory conditions have been measured by optical or SIMS means.

The rim of lab hydrated samples show that the thin sectioned microscopic optically measured depth is less than the actual depth indicated by H^+ profiles by SIMS that implies optical underestimates true depth (Novak & Stevenson 2012; Stevenson et al., 2002). Any hydration rim data should be compared to the Optical versus SIMS plot to get a true depth rim**.** The full width half maximum (FWHM) point is taken at the inflection point of the later part of the SIMS H^+ profile for the SIMS data (**APPENDIX Fig. A1**). Using the end point of the tail in SIMS H+ profiles is misleading and is avoided; the obtained equations have not produced an acceptable dating result.

Due to the lack of calibrated image data of aged samples but from BH1, depth / year was mostly employed in the power law fanction.

3.1 Power law of the five high T Experimentally aged obsidians

Table 1 gives power law equation for the five sources at high temperatures as $Y=C*X^p$, where Y =rim/yr or Pixels/yr, X = Temperatures in x20 and x60 magnification, p the exponent. The exponents p, vary with Depth/yr between 3.7 – 3.9 (excluding NZ); the Pix/yr (x20) varies 4.4-4.8 excluding NZ, and the Pix/Yr (x60) between 4.7-5.0 excluding NZ.

It seems the μm/year has a lower average of exponents 3.7-3.9. The former 3.7 occurs with low water (Peru, BH1). The latter 3.9 occurs for high water (Mexico, BH2, except NZ).

The Pixels/year have a higher average between 4.3-5.7 but without any obvious trend, yet a tendency of lower and higher exponents of low and high water respectively.

Table 1 Power law of five sources at high temperatures only as microns/yr and pixels/yr in x20 and x60 magnification. * BH1 rim data used in Liritzis & Andronache, (2024 Part I), provided by A.K. Rogers (Rogers et al., 2022a) were slightly different, leading to a different equation; the re-measured ones by C.M.Stevenson are quoted here.

PERU, 0.11%	**NZ, 0.21%**	**MEXICO, 0.21%**	**BH1, 0.10%***	**BH2,0.25%**
Depth /Yr				
$y = 8E\text{-}07x^{3,7152}$	$y= 2E\text{-}11x^{5.701}$	$y = 2E\text{-}07x^{3,9141}$	$y = 5E\text{-}07x^{3,717}$ R=0.99	$y = 1E\text{-}07x^{3,946}$,
$R^2 = 0,9953$	$R^2 = 0.992$	$R^2 = 0,9984$		R=1
AVERAGE all: $Y =4E\text{-}08*X^{4.2}$				
AVERAGE without NZ: $Y =(4E\text{-}7\pm 3,16E\text{-}07)*X^{(3.82\pm0.124)}$				
Pixels/Yr (x20) without scale (cannot calculate areas)				
$y =0,001x^{4,3809}$	$y = 4E\text{-}08x^{6,2502}$	$y = 8E\text{-}05x^{4,8414}$	$Y=0.0006*x^{3.2}$, $R^2=0.92$	No images, only
$R^2 = 0,9846$	$R^2 = 0,9942$	$R^2 = 0,9779$	We do not know scale	rims
Pixels/Yr x60 with scale				
$y = 0,0008x^{4,6658}$	$y = 3E\text{-}06x^{5,64}$,	$y = 0,0001x^{5,0095}$	No images	No images
$R^2 = 0,9991$	$R^2 = 0,9583$	$R^2 = 0,9982$		

The five sets followed the Power law. The three different sources in depth/year gave interesting numbers for exponents. The NZ Hahei source has a little higher exponent of 5.7. The fitted curve was not consistent with the law and the predicted values were a bit far away from actual values this might be due by the variable NZ hydration duration 30-80 days.

The exponents and coefficients of the five sources varied between 3.7-3.9 and E07 respectively, but NZ 5.7 and E-11. In pixels these values are spread a bit more (3.2-6.2 for x20 and 4.6-5.6 for x60; and the area/yr x60 between 4.9-5.6.

For low water samples (Peru, BH1) exponents are similar and coefficients 8E-07, 5E-07.

High water samples (NZ, Mexico, BH2) exponents are similar 5.7 (NZ), 3.9, 3.9. The coefficients are 2E-011 (NZ), 2E-07, 1E-07. NZ is out of an expected relationship.

Example: Using the Mexican function Rim/yr = $2E\text{-}07*T^{3,9141}$ for EHT=12°C, and the calculated value um/yr=0.0033, then, if rim of unknown sample is 4 um, the calculated age from Table 1 for Mexico is 4 um / 0.0033 um/yr=1212 years BP. However, relying on the high T power law is not reliable because the lower T region does not exhibit similar diffusion kinetics; hence the equation is enriched with environmental T aged obsidians, as reported below.

Water versus power law

A plot of the 4 sources excluding NZ hydration of water (as OH%) content and exponent, coefficients gave a linear relationship (Fig. 1). Both exponent and coefficient of Power Law have a functional dependence with intrinsic water OH%.

Of interest is the overlapping Peru and BH1 points of sources with similar pristine water content but different coefficients. This recalls the linear relationship between energy (E) and water content (as OH%). The Fig 1 (a, b) plot was to explore any dependence on exponent and coefficient Vs water content.

Although we believe that the structural variation of sources concerning pristine water content, pores sizes, type and size of crystalline phases, mechanical properties, attributes a unique power law per source, small changes between them do not affect considerably the coefficient and exponent of the functional equation.

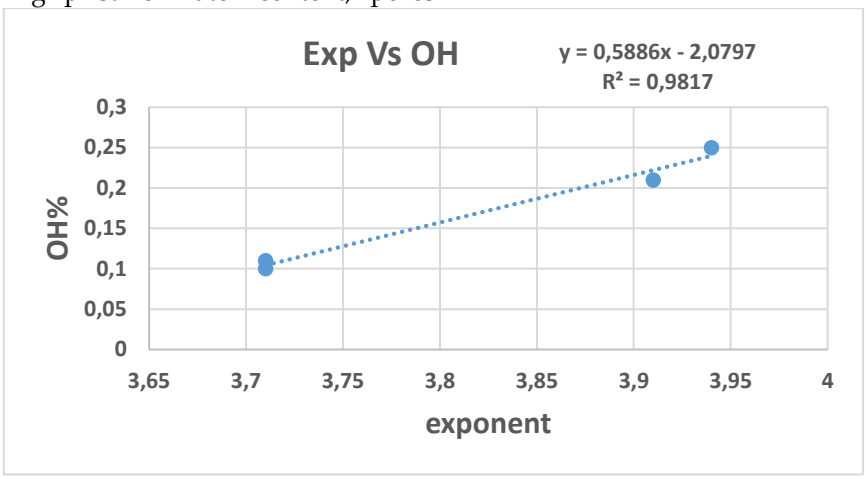

(a)

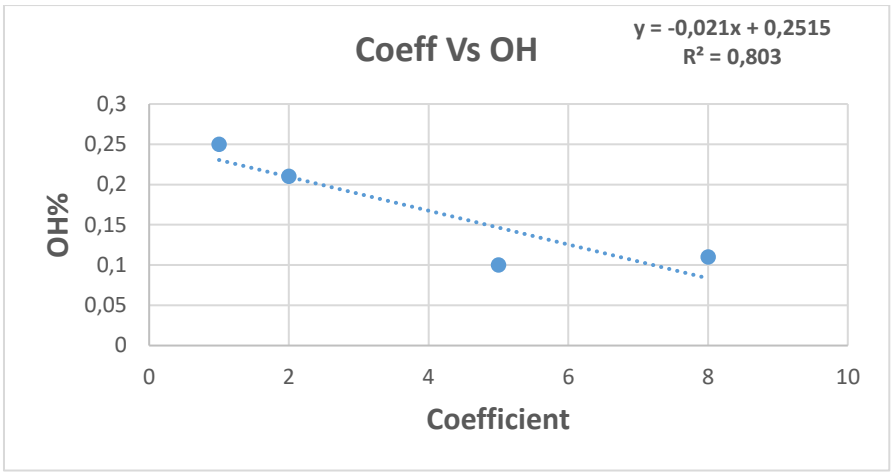

(b)

Figure 1: OH% versus a) power law exponent and b) power law coefficient of power law of Table 1 (excluding NZ).

However, the different OH% between obsidians (see BH1 and BH2) for same T and applying the Power Law equation constructed by the five high T aged experimental data and the four low T from Umleang, provide slight differences in age estimation despite the water% difference (**APPENDIX Fig.A2**).

3.2 Power law of the nine aged Obsidians at five high and four low T from Umleang

The data used is in Table A1 (supplementary). The power law here includes nine aged obsidians: five in high (140-180^{o}C) and four in low -environmental or archaeological- (10-40^{o}C) temperatures (Table 2). This Table includes high and low T data, while Table 1 is for high T data only. (see **APPENDIX Fig.A1**).

The low water samples (Peru, BH1) give close in numbers exponent 5.9, 5.6 and order of magnitude coefficients 1E-11 and 2E-11.

The high-water samples (NZ, Mexico BH2) give exponents 3.81, 5.75 and 5.65 and coefficients 2E-11, 2E-07. It is striking the similar exponents but for NZ. The NZ data have been different in other combinations too; that lead us to either exclude NZ or accept separately these data. In any case including or remove NZ the average exponent varies - in the case of all data of Table 2 it varies in the decimal point of number 5, and in the case of only High T data of Table 1 close range difference of 4.2 and 3.8.

Table 2. Power law (um/yr Vs T) for five (New Zealand, Peru, Mexico, California) with respective water content and four low T from Umleang (H2O 0.10%), New Guinea, as microns/yr. Reconstructed: extrapolating Power Law of high T to 10-40°C.

PERU, 0.11% +Uml	NZ, 0.21% +Uml	MEXICO, 0.21% +Uml	BH1, 0.10% +Uml	BH2,0.25% +Uml
Depth /Yr				
$y = 1E\text{-}11x^{5,9307}$	$y = 2E\text{-}07x^{3,8157}$	$y = 2E\text{-}11x^{5,7485}$	$y = 2E\text{-}11x^{5,6343}$	$y = 2E\text{-}11x^{5,6549}$
$R^2 = 0,9556$	$R^2 = 0,9655$	$R^2 = 0,9727$	$R^2 = 0,992$	$R^2 = 0,9596$
	Reconstructed: $y = 3E\text{-}11x^{5,6185}$ $R^2 = 0,9976$			

Average of All high T Sources + Uml: $Y = 2E\text{-}10*X^{5.357}$
Average of All high T Sources + Uml without NZ: $Y = 2E\text{-}11*X^{5.742}$
High T power law (Table 1)
AVERAGE all high T only sources: $Y = 4E\text{-}08*X^{4.2}$
AVERAGE of all high T without NZ: $Y = (4E\text{-}7 \pm 3,16E\text{-}07)*X^{(3.82\pm0.124)}$

A characteristic plot for the Peru and New Zealand with Umleang data is given in Fig.2. The Y-axis is in units of um/year instead of um²/year because we used the rate given from experiments, i.e. rim per experimental time. The curve in Fig. 2 -the high T data coupled with low T data- fits with power law. The seemingly linear is visually misleading. For example, at the high T part of the power law observe that data could "seem" linear but are not. It is not T Vs um but, T Vs um/year.

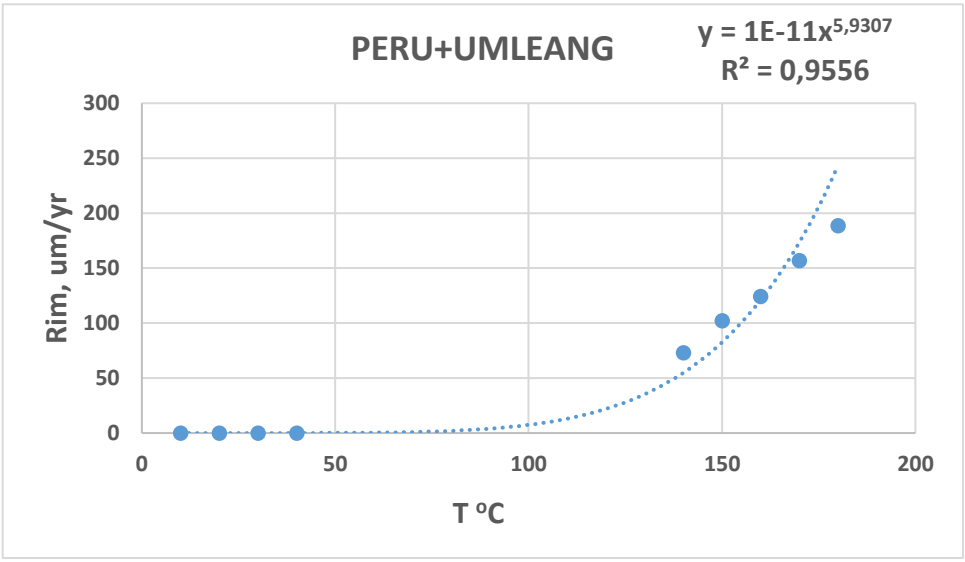

(a)

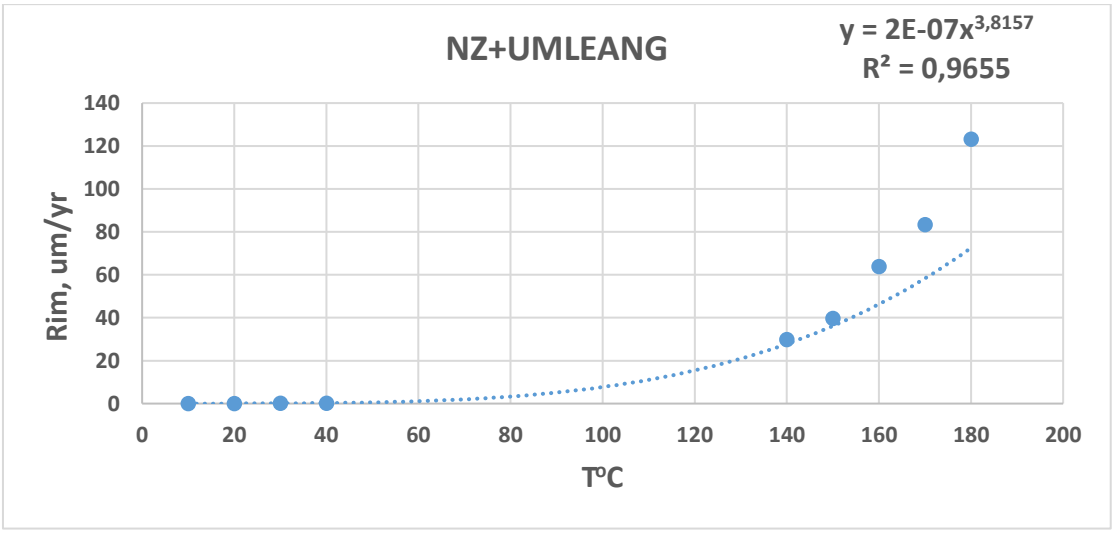

(b)

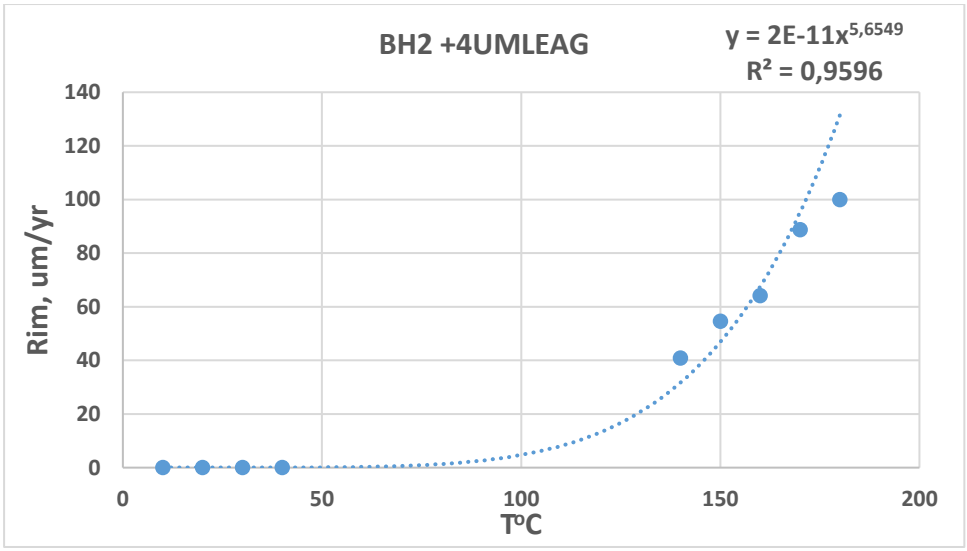

(c)

Figure 2: a) Power law of the Peru and b) New Zealand and c) (high T) including Umleang (low T) data.

3.3 Power law of the nine aged Obsidians at five high and four low T from Wekwok

The second set of low temperature aged obsidian from Wekwok gave also the power low (Table 3). It is striking the fact of the exponent 3.74 which is at same variance to the power law for the five aged at high T sources with the average 3.82 without NZ, but different compared to respective Umleang data with same five sources (5.36).

Table 3. The power law (um/year versus T) for the high T sources and Wekwok (0.10% H2O) low T data.

BH2 0.25%OH +Wek	BH1 0.10%OH +Wek	NZ 0.21% +Wek	MEXICO 0.11% +Wek	PERU 0.11% + Wek
$y = 1E\text{-}07x^{3,946}$ $R^2 = 1$	$y = 5E\text{-}07x^{3,717}$ $R^2 = 0,999$	$y = 8E\text{-}07x^{3,5329}$ $R^2 = 0,9547$	$y = 5E\text{-}07x^{3,6629}$ $R^2 = 0,9992$	$y = 3E\text{-}07x^{3,845}$ $R^2 = 0,9986$

Average of all high T sources + Wekwok: $y = 4E\text{-}07x^{3.74}$

***

Average of All high T Sources + Uml (Table 2): $Y = 2E\text{-}10*X^{5.357}$
Average without NZ: $Y = 2E\text{-}11*X^{5.742}$

The equation for similar water content (BH1, Mexico, Peru, Wekwok) gives exponents p=3.72, 3.66, 3.84 and coefficients 5E-07, 5E-07, 3E-07. This is a very encouraging result of close values, knowing the correlation of water content to rates, with occurred differences probably due to other causes, e.g. chemistry and mechanical properties of the different sources, statistical errors in ageing experiments. The same explanation may apply to the two high water equations of Table 3.

3.4 Provisional dating of archaeological samples

The computed diffusion rates as microns / year of the aged obsidians correspond to the laboratory-controlled low temperatures which are taken as the EHT.

The power law between the hydration rim and time is related to the diffusion rate k (see eq.2, 3). The latter is contingent to the structural and chemical content and water presence of each volcanic obsidian source (Liritzis and Andronache, 2024c, in preparation). Bearing in mind this dependency, a provisional examination of the present equation to deduce OHD ages is made for some well dated samples of known age and estimated EHT.

Table 4 (A) gives a detailed example of the time intervals for respective temperature ranges of calculated Easter Island ages using power law equations of respective obsidian source and low temperature data from Umleang New Guinea. Table 4(B) presents the calculated and reported ages and temperatures for all tested dated samples. The equations used are representative of all produced in Tables 1,2,3.

For Easter Island the various combined data for constant T gives an age range of ±10% from average. Using only Power Law of higher T data (um/year versus T) the ages are wrong. For the rest of dated

samples there is not a trend where an equation is applicable to all. The equations of some combinations of different sources give dates consistent with those reported in the literature, others give non meaningful ages. A degree change in the EHT has a profound result in age. The water content of dated samples does not seem to correlate with the equations derived from the respective water content. A tendency is observed of Papua and Japan samples approached by NZ equation.

A few comments per sample case are provided below.

*Table 4. Easter Island ages. a) Graphical presentation of the time intervals for respective temperature ranges of calculated Easter Island ages using power law equations of respective high T obsidian source and low temperature data from Umleang New Guinea (Table 2) for one of the rims 1.41um. Red is the T range from the reference. BH2 (hT) denotes only the high T power law, b) Calculated and reported ages and temperatures of equations including all high T sources with Uml or Wek, from Tables 2, 3. Reported ages usually are cal. C-14 dates and temperatures are EHT (see references in the text). In columns ages of combined power law equation / temperature range. nm=not meaningful usually too low. * The sample is of late Glacial period and average T is less than today or Holocene see text). All sources of low water content (0.10%), except OCH and Ethiopian (0.18-0.20%).*

(A)

T°C→	**21**	**21.5**	**22**	**22.5**	**23**	**23.5**	**24**	**24.5**	**25**	**25.5**	**26**
Equations						**A g e s, BP**					
BH2(hT)						50-90					
BH2+Uml	2500	2250	1922	1690	1494	1360	1175	1000	932	850	747
BH1+Uml	2662	2300	2048	1800	1594	1400	1254	1100	996	900	800
Peru+Uml		1880	1640	1450	1260	1100	978	810	760	1400	600
Mexico+Uml	1880	1640	1440	1260	1115	990	872	770	690	620	550
NZ+Uml		1630	1430	1260	1117	1000	880	790	700	630	560
Sample age range		**1600**							**600**		

(B)

Samples (with µm)/Ages per temp.	**Reported Age, years BP/Temp °C**	**Av all. With Umleang (Table 2)**	**Av all with Umleang, no NZ, Age BP/Temp.°C**	**NZ+Umleang**	**Av. All+ Wekwok (Table 3)**	**NZ+Wekwok**	**NZ rec.**	**Peru Rec.**	**BH1 Rec.**	**BH2+Umleang**
Papua, 10.49	**7,732±89 / 25**	nm	7,900-3,200 /23-27	nm	nm	nm	7800-4000 / 23-26	nm	nm	7313-6524 / 24.5-25
Papua, 11.82	**10,883-10,365 / 22-23**	11,000-8,300/18-19	9,800 ±700 / 22-23	nm	nm	nm	11,300-8,800 / 22-23	nm	nm	15146-11780 /22-23
Papua, 12.5 (by extrapolation)	**14,000 / 27**	16,000-12,000/17-18	11-14,000 / 21-22*	nm	nm	nm	15,500-12,000 / 21-22	nm	nm	5031-16050/ 27-21
Ester Island, 1.5	**1100-550 /21.9-22.2**	nm	1918-500 /21-26	nm	nm	nm	1434-560 /22-26	nm	nm	1972-1826-1175/21.9 -22.2-24
Japan, OCH, 2.73	**~4,700/7.94**	nm	nm	5,900-4,370 / 6.9-7.5	4700 / 7	6,000-3,500 / 6-7	nm	4,300/ 6	6,800-3,900/ 6-7	nm
Japan, SHIR, 4.8	**17-19,000/8-9**	nm	nm	24,000-10,000/ 5.5-7	20,000-8,300/ 5.5-7 (14,500/6)*	nm	14,300-8,600 / 7-8	15,000/ 5	17,000-12,000/ 5.4-6	nm
NV, 1,9	**472/17.15**	nm	nm	400/15	nm	nm	nm	nm	450/11.5	nm
NV, 4.5	**2650/ 16.23**	2760/19.5	nm	2000/11.5	nm	nm	nm	nm	nm	nm
NV 7.7	**7750/ 15.76**	7260/ 18	nm	nm	nm	nm	nm	nm	nm	nm
Ethiopian 1, 46.99	***LSA/MSA (60-70,000)/20?**	25,000-19,000/20-21	79,000-46,000/ 20-22	nm	nm	nm	76,000-45,000/20 -22	nm	nm	103246-60230/20-22

Samples from respective locations of Table 4 may apply those power law equations that produce satisfactory dates in our examples. The most problematic is the NV data.

Easter Island

Maunga Tari (Stevenson, 1993): Applying the five equations per source and for Umleang low T, Table 4a is obtained with age and temperature ranges for various power law equations. The overlapping dates in years BP are shown for the interval ~600-1600 years BP of the sample age span in temperature span 21-26°C (see Liritzis and Andronache, 2024c). Though the age range is correctly defined, the 1-3 °C higher T may be due to the different obsidian sources of Easter Island sample and calibration sources.

From Table 4b none of the power law equations gave meaningful results. Satisfactory data were those of the average all four sources (Peru, Mexico, BH1, BH2) + Umleag data for low temperature region (excluding NZ with a different exponent 5.8); also, the NZ reconstructed curve consisting of high temperature aged power law and for low (10-40°C) the calculated derived ones (exponent 5.6, Table 2).

Two Japanese

a) Ocharasenai site, ~4,700 years BP for EHT=7.94°C (Nakazawa 2016): Concordant results were obtained with NZ+Umleang curve, 4,300-5,900 BP for 6.9-7.5°C; with all sources + Wekwok low temperature data, 4700 years BP for 7°C and with Peru reconstructed low temperature data of 4,300 years BP for 6°C and the BH1 reconstructed gave 3,900-6,800 BP for 6-7°C.

b) Kyo-shirataki 3 (Hokaido) 17-19,000 yrs cal C-14 BP, for EHT=8.1°C (Nakazawa 2024, pers. Comm.). Interesting results were obtained but for EHT lower than quoted, because the burial period covers Holocene and Late Glacial. Today the average T in Hokkaido is 5°C. The NZ+Umleang data curve gave 24,000-10,000 years BP for 6.9-7.5°C; the Average Wekwok 20,000-8,300 years BP for 5.5-7°C (14,500 BP for 6°C); the NZ, Peru and BH1 reconstructed gave dates of Late Glacial for 5-8°C.

We note that the two Japanese samples gave ages close to the C-14 for T around the estimated EHT. Bearing in mind the Polynesian-NZ volcanic area that characterize the power law from this region, and the different Japanese sources to be dated, the calculated temperatures are very close for the anticipated dates.

Papua samples

Several ages were calculated in a stratigraphic order as shown in Fig.3.

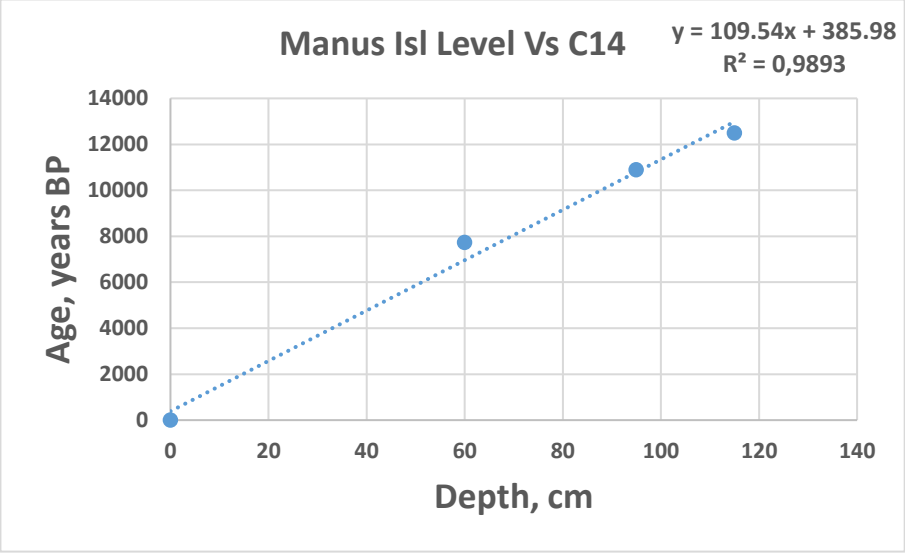

Figure 3: Stratigraphy from which the 125cm depth samples date of ~14,000 cal C-14 years BP was deduced, as the extrapolation of the curve (corresponding to an average hydration rim of 7 rims of 12.5um).

For the 10.49 um sample the Average sources +Umleang gave 7,900-3,200 BP for 23-27°C and, with NZ reconstructed the age of 7,800-4,000 ears BP for 23-26°C.

The other sample at 11,82 um of 10,883-10,365 BP cal. C-14 at 95cm depth and 22-23°C, gave via the Average Sources no NZ + Umleang the date of 9,800±700 years BP for 22-23°C; then 11,000-8,300 BP /18-19°C with Average of all Umleang; and with NZ reconstructed 11,300-8,800 years BP / 22-23°C.

The last sample 12.5 um, as with the former one, the same three power law equations were most proper with age ranges: for Average all sources no NZ + Umleang the 16,000-12,000 years BP for 17-18°C;

then 16,000-12,000 years BP /17-18^{o}C with Average of all Umleang; and with NZ reconstructed 15,500-12,000 for 21-22^{o}C. Calculated ages beyond the defined temperatures were far away of the C14 dates of the respective layers.

Last For 125cm depth which is the extrapolation of the curve (Depth Vs C14) above the average of 7 rims is 12.5 um. This corresponds to 14,000 cal. C-14 years BP from the linear curve above.

Napa Valley

The three Napa Valley samples are most tentatively used as they incur uncertainties on their exact burial depth.

The NV 1.9um of ~472 BP / 17.15^{o}C the NZ+Umleang power law gave ~470 BP for 12.5^{o}C and ~450BP for 11.5^{o}C; both ages similar to the reported but with lower temperature.

The NV 4.5um did not produce meaningful result and the NV 7.7um/15.76^{o}C only the Average all sources +Umleang gave 7,260 years BP for 18^{o}C.

The NV 7.7 at 90-100cm, 7750 years, EHT=15.76^{o}C, gave for the Average all + Umleang 7260 BP for 18^{o}C.

Ethiopian

During the time of the Last Glacial maximum in high latitudes, temperatures are known to have been at least 6^{o}C lower than they are today Clark et al (1984) the EHT=24.8oC; including LSA Temp < 24.8oC, we get on average 18-24oC or ~20±1oC).

The calculated age range using the Average of all sources + Umleang was 25,000-19,000 years BP for 20-21^{o}C; applying the average of All sources no NZ + Umlean g gave 79,000-46,000 years BP for 20-22^{o}C, and with the reconstructed NZ the age obtained is 76,000-45,000 years BP for 20-22^{o}C.

We have observed that the pixels/year parameter versus T equation introduced earlier (Liritzis and Andronache, 2024, Part I), gave satisfactory ages, despite the different rim data. As was noted "…. *the ages with power law of BH of T Versus pixels/yr, non-normalized (800*600 pixels image size for Ethiopian blades), vary between around 1,200 to 45,000 years BP. In same time BH images were normalized from 320*240 to 1429*1072 pixels image size of NV, too, and the ages ranged between 7,000-280,000 years on these normalized values to NV for temperatures 10-31^{o}C (Table 8). For the latter for 15-17^{o}C (most probable) the calculated ages are 46-69,000 years for PE-21 and 51-76,000 for PE23. One can realize here the compulsory normalization in such dating calculations…*".

We have proved that the pixels areal quantity during diffusion includes environmental parameters which impact diffusion rate and T variation from the succolarity index and fractal dimension. As stated earlier (Liritzis et al., 2024b), "*....we found that especially the succolarity, which is based on the capacity of a water fluid to percolate through the obsidian area in a given direction, was critical to determine the characteristics of the obsidian hydration layer. The FFI and LCFD estimate the compaction/fragmentation and connectivity, respectively. Therefore, the fractals play an important role in understanding the general diffusion in solids theory and the study aims at providing a new direction in the OHD and diffusion fields concerning the complex dynamic systems and structures which display a fractal pattern*".

DISCUSSION

The prevailing functional dependence of the temperature with hydration rim per time in all aged experiments of obsidians from different volcanic sources in the World is the power law. The exponents lie on average between 3.2 and 5.5. The coefficients of the equations exhibit uniformity; all sources with Umleang except NZ and the high T of NZ and NZ reconstruction have E-11, all high T with Wekwok of the order of E-07.

Obviously, Igneous rocks look different based on many different compositions, depending on the magma they cool from and on their cooling conditions, while each volcano and its eruptions are unique.

Regarding plate tectonics and the Ring of Fire, the latter is a string of volcanoes and sites of seismic activity, or earthquakes, around the edges of the Pacific Ocean. Along this ring are situated the obsidian sources investigated, with the Easter Island at the edge Volcanic Puzzle in the South Atlantic and with both with New Zealand to sit at the edge of this volcanic ring[2] (Moore 2012; Mitchell 1989; Holm et al., 2023).

Even though the fitting of experimental data may inhere some uncertainties (instrumental, environmental, procedural, experimental setting, and human) beyond the gaussian experimental errors, we believe that the obtained consistent power law should represent a global validation with similar numerical exponent and coefficients. Their variation due to the local sources may appear at the last integer of the coefficient of same number of decimal points and the slight change in the exponent. Concerning the reported pristine water (H2Om and OH) linear dependence from activation energy E and rate, k (Rogers 2008b; Rogers and Stevenson, 2022a, b; Stevenson et al., 2019) or power law dependence for a greater range of water % (Liritzis and Andronache, 2024c), it has

[2] https://education.nationalgeographic.org/resource/plate-tectonics-ring-fire/

been observed such a linear relationship with the exponents and coefficient of power law equations. But we have not observed any convenient use of a particular power law equation based on this relationship.

The role of structural water has been reported in un-hydrated bulk obsidian and has been found to have a strong correlation with the pre-exponential and activation energy, allowing for the estimation of the Arrhenius constants. Moreover, the analysis of hydrated Napa Glass Mountain obsidian using secondary ion mass spectrometry (SIMS) at 90°C demonstrates that the initial diffusion stages display a dynamic behavior characterized by fluctuating hydrogen levels and a decreasing diffusion coefficient over time (Stevenson and Novak, 2011).

These research endeavors have significantly enhanced our comprehension of the process of glass hydration and alteration and have identified crucial factors to be considered when simulating water diffusion in glass at archaeological locations throughout the years.

Regarding the functional dependence earlier low temperature hydration experiments at 75°C on Pachuca obsidian from Mexico show that the diffusion coefficient of hydrogen within the developing hydrogen profile does not follow a square root of time dependence. In addition, hydration rates calculated using $t^{1/2}$ or t^{1} do not result in extrapolations to zero hydration when samples are linked to contexts of known age. Considering this situation, critics of the $t^{1/2}$ model prefer to use a t^{n} format where n is the best fit regression coefficient from the experimental data (Stevenson and Novak, 2011)

The power law of microns versus temperature is preferred to power law of pixels versus T because does not import image sizes and hence no normalization is required. In the initial diffusion the rate is not of the same order as in longer hydration times explained by the quadratic dependence of diffusion with time and the power law found here. It has been reported that the near to surface saturation layer provides a virtually new start of diffusion that eventually makes the variation of water to follow two mechanisms, one based on Fick's law and another exponential like that tends to zero at the hydration tail (Brodkey and Liritzis, 2004; Liritzis, 2006).

The present novel research makes a significant contribution to the academic field of the diffused obsidian and its hydration dating.

The high temperature experiments made in the past to accommodate data in the Arrhenius plot and estimate the diffusion rate at ambient (burial) temperatures, together with low temperature aged experiments, seem to provide satisfactory hydration rims (measured by optical or SIMS means). The product of the hydration depth is the result of an average diffusion rate kinetics behavior during the archaeological time and average temperature since its production/usage time and burial history of an obsidian artifact. This combined outcome depicts the obtained power law function which, with reasonably estimated environmental temperature values (or EHT) and respective obsidian source, may provide an alternative approach in OHD.

The limitations of the power law on pixels image data dating lie in the manner of taking images by microscopes their magnification and resolution (hence normalization is always recommended), the EHT estimation (burial history), and questions on accuracy of rim measurements from especially older reported data.

The present investigation gave encouraging results which derive from seven obsidian sources and artifacts from different geographical regions.

The rim of laboratory hydrated samples show that the thin sectioned microscopic optically measured depth is less than the actual depth indicated by H^{+} profiles by SIMS that implies optical underestimates true depth (Novak & Stevenson 2012; Stevenson et al., 2002).

The experimental results of the rate in hydration behavior of glass/obsidian/cemented systems been investigated over the temperature range 10° to 80°C hydration at 60°C and 80°C under different water/solid ratio values have shown that not only hydration kinetics are strongly temperature-dependent, but that also hydration occurs through another mechanism: a near-surface (topochemical) and a through-solution mechanism following Fick's model (Brodkey and Liritzis; Dova et al., 2005; Stevenson et al., 2024). The water/solid obsidian ratio changes imply dissociation of water, and water connected to amorphous Si-lattice, to OH radicals, which in turn indicates variation in the solubility paths (pores etc.). The latter depends clearly on temperature, pressure, the type of bond and forces between the particles changing the available voids, the structural characteristics of each obsidian source, are few among them. Already we have observed a proportional variation between rate k and growth rate um/year for the 10-30°C, and an expected non-liner change for higher temperatures (**APPENDIX, Fig.A3**).

An earlier test of k dependence of eq.3 on E and T as percentage error of the ratio $1/\exp(-E/RT)$ for different activation energies from 20 kJ/mol up to 90 kJ/mol and for ±5 °C in temperature deviated from 20 °C shows a striking result from few % to considerable % changes (Liritzis and Laskaris, 2011, Fig.3).

The dated samples derive from sites and areas where we had no available power law from similar source. The near to archaeological sites obsidian

sources are for California (NV sites and BH1, 2 volcanic rocks). The New Zealand and New Guinea sources with Papua site. The rest of the sources (California, Mexico, Peru) produce representative curves per volcanic source. The variation of the power law curves is due to the coefficient and exponent values- the former in the last decimal integer or the order of thousands as E-07 or E-11, and the latter between ~3-5.

The obtained ages using various forms of the Power law are indicative yet promising for a calibrated curve per volcanic source to circumvent the uncertainties from the use of proxy or distant sources.

The low temperature aged data (at least the10-30°C) which simulate possible environmental conditions, cannot be used as unknowns in the present research and only high and low temp data from same source would be ideal for most accurate dating. But the satisfactory ages we have obtained under mixed sources of high and low T aged data power law equations gives a hopeful direction for current OHD trend.

Furthermore, the relationship between the k rates was examined from eq.1 amongst 9 dated samples (Fig.4a). The variation of rates is expected and the similarity of same sources (NV) expected.

Then the k was plotted with LnT (of reported EHT) (Fig.4b) and extrapolated to lower T (Fig.4c).

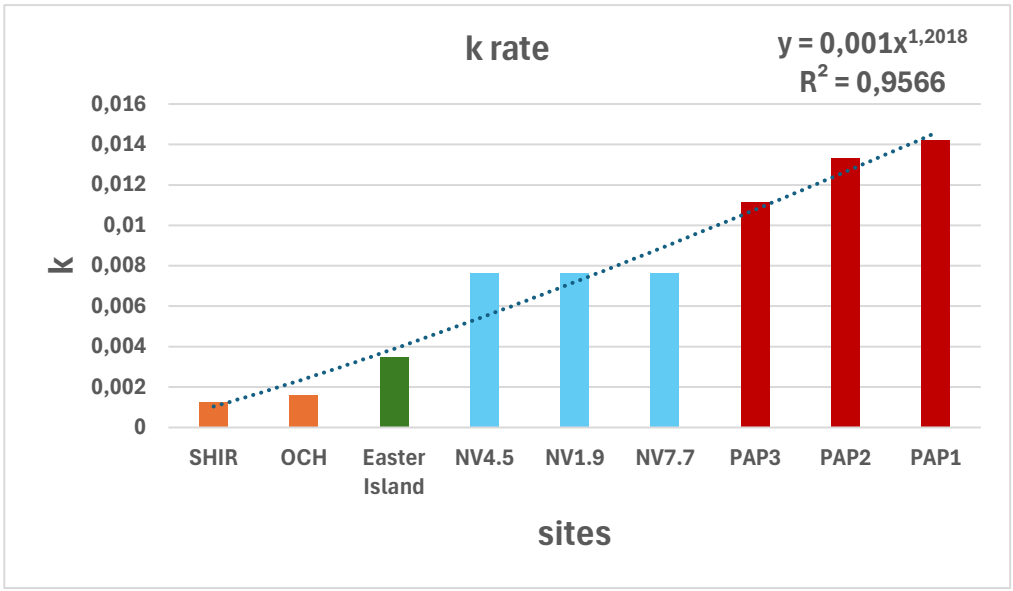

(a)

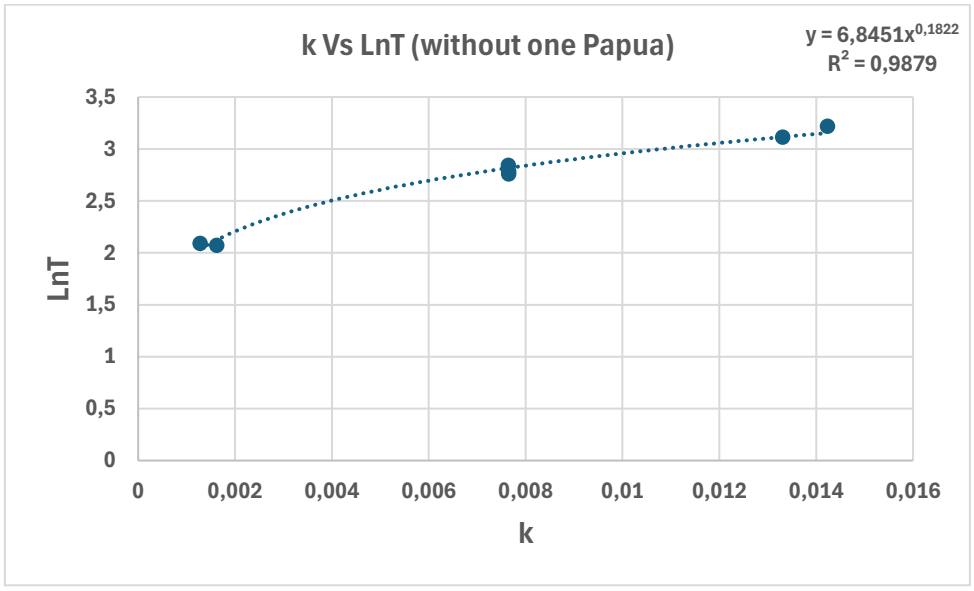

(b)

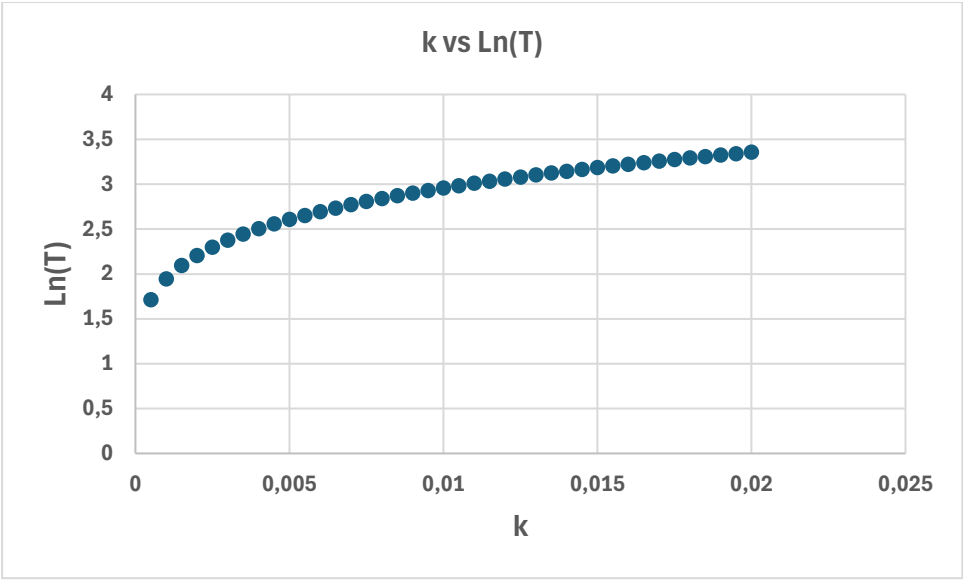

(c)

Figure 4: a) The k value of rate versus the 5 sites and 9 dates, b) k from (a) versus LnT. The Papua sample of 12.5 um was excluded, c) as (b) for developing the power law at low temperatures.

We notice a power law behavior in Fig.4b but the variation in T affects the K and hence age, due to the susceptible dependence of hydration rim development with temperature. In the Papua case of 12.5 um the ages obtained for T=17-27°C range 18,300 to 8,500 years BP respectively, almost like results of Table 4b.

Summarizing, following up the first report of the power law approach (Liritzis and Andronache 2024a), it is now proven that this alternative approach is an essential development of OHD. Especially, the areal pixels / year of the hydration layer images, have a physical meaning connecting complexity measures of fractal dimension[3] with the water percolation through obsidian surfaces. The power law describes the diffusion by, in addition to rim / year, the more representative agent of pixels per year versus T.

Its potential contribution to the understanding of water diffusion process in obsidians from various volcanic environments affirms the sensitive role of EHT and the prominent direction of image analysis for age calculation.

CONCLUSION

The functional dependence of obsidian diffusion temperature with hydration thickness and pixels is investigated using experimentally aged data at high temperatures (140–180 °C) from five globally distributed obsidian sources (California, Mexico, Peru, and New Zealand) and at low temperatures (10–40 °C) (New Guinea). The power law equations used are from the respective obsidian source high and low T ageing experiments such as depth/time or pixels of hydrated layer/time against temperature.

In all ageing studies with obsidians from various volcanic sources worldwide, power law is the dominant functional relationship of temperature with hydration rim per time. On average, the exponents fall around 3.2 and 5.5. The coefficients of the equations show homogeneity- all sources with Umleang have high T with Wekwok in the order of E-07, except for New Zealand (NZ), and the high T of NZ and NZ reconstruction has coefficient E-11. The variable NZ hydration duration 30-80 days may be a source of causing inconsistencies.

Naturally, every volcano and its eruptions are unique, and the composition of igneous rocks varies greatly depending on the cooling conditions and the magma from which they condense.

It has been shown a power law pattern, but because hydration rim development is vulnerable to temperature changes, changes in T have an impact on hydration rate (k) and, consequently, age.

To avoid the errors associated with employing proxy or distant sources, the ages derived using different versions of the Power law are promising but indicative for a calibrated curve per volcanic source. Only high temperature data from the same source would be ideal for the most reliable dating, because low temperature aged tests cannot be used as potential EHTs in the current study. However, the acceptable ages we have determined using the power law equations for mixed sources for specific regions provide a positive outlook for the present OHD trend.

[3] Succolarity, lacunarity, correlation dimension, local connected fractal dimension (LCFD), fractal fragmented index (FFI), entropy and normalized Kolmogorov complexity (TIFF-LZW).

Authors contribution: Conceptualizing: I.L.; methodology, I.L., I.A.; software, I.A., I.L.; validation, I.L., I.A.; formal analysis, I.L., I.A.; investigation, I.L., I.A.; data curation, I.A., I.L.; writing—original draft preparation, I.L.; writing—review and editing, I.L., I.A.; visualization, I.L., I.A.; supervision, I.L.; project administration, I.L. Both authors have read and agreed to the published version of the manuscript.

Acknowledgements: We are thankful to Prof. Chris M Stevenson for his support with data provision and discussion and constructive comments on the manuscript, Prof. A.Rogers for useful data on temperature, Dr Tom Origer& Associates, for data provision and reading the manuscript and Steven Brant, University of Florida, for providing some obsidian samples.

REFERENCES

Ambrose, W.R. (1994) Obsidian hydration dating of a Pleistocene age site from the Manus Islands, Papua New Guinea. *Quaternary Science Reviews*, Vol. 13, 137–142. https://doi.org/10.1016/0277-3791(94)90039-6.

Ambrose, W and Noval, S.W. (2012) Obsidian hydration chronometrics using SIMS and optical methods from 26-year temperature-controlled exposures. In: Liritzis, I and Stevenson, C.M (eds), *Obsidian and ancient manufactured glasses*, Chapter 2 15-25, University of New Mexico Press, Albuquerque, USA.

Ambrose, W., Novak, S.W., Abdelrehim, I. (2004a) Powdered obsidian for determining hydration rates and site thermometry. *Mediterranean Archaeology and Archaeometry*, Vol. 4, No 2, 17–31.

Ambrose, W.R., Stevenson, C.M. (2004b) Obsidian density, connate water and hydration dating. *Mediterranean Archaeology and Archaeometry*, Vol. 4, No 2, 5–16.

Anovitz, L.M., Cole, D.R., Fayek, M. (2008) Mechanisms of rhyolitic glass hydration below the glass transition. *American Mineralogist*, Vol. 93, 1166–1178. https://doi.org/10.2138/am.2008.2516

Anovitz, L.M., Elam, J.M., Riciputi, L.R., Cole, D.R. (2004) Isothermal time-series determination of the rate of diffusion of water in Pachuca obsidian. *Archaeometry*, Vol. 46, 301–326. https://doi.org/10.1111/j.1475-4754.2004.00159.x

Anovitz, L.M., Riciputi, L.R., Cole, D.R., Gruszkiewicz, M.S., Michael Elam, J. (2006) The effect of changes in relative humidity on the hydration rate of Pachuca obsidian. *Journal of Non-Crystalline Solids*, Vol. 352, 5652–5662. https://doi.org/10.1016/j.jnoncrysol.2006.08.044

Brodkey, R., Liritzis, I. (2004) The dating of obsidian: a possible application for transport phenomena (a tutorial). *Mediterranean Archaeology & Archaeometry*, Vol. 4, 67–82.

Clark, J.D., Williamson, K.D., Michels, J.W., Marean, C.A. (1984) A Middle Stone Age occupation site at Porc Epic Cave, Dire Dawa (east-central Ethiopia). African Archaeological Review, Vol. 2, 37–71. https://doi.org/10.1007/BF01117225

Crank, J. (1976) *The mathematics of diffusion*. 2nd ed., Clarendon Press, Oxford.

Doremus, R.H. (2002*) Diffusion of reactive molecules in solids and melts*. J. Wiley & Sons, New York.

Doremus, R.H. (2000) Diffusion of water in rhyolite glass: diffusion–reaction model. *Journal of Non-Crystalline Solids*, Vol. 261, 101–107. https://doi.org/10.1016/S0022-3093(99)00604-3

Doremus, R.H. (1969) The diffusion of water in fused silica. In: Mitchell, J.W. (Ed.), Reactivity of Solids, Wiley, New York, pp. 667–673.

Dova, M., Palou, P., Kovar, V. (2005) Heat evolution and mechanism of hydration in CaO–Al2O3–SO3 system. *Ceramics- Silikáty*, Vol. 49, 104–108.

Fernández, V.M., De La Torre, I., Luque, L., González-Ruibal, A., López-Sáez, J.A. (2007) A Late Stone Age sequence from West Ethiopia: the sites of K'aaba and Bel K'urk'uma (Assosa, Benishangul-Gumuz Regional State). *J. African Arch*, Vol. 5, 91–126. https://doi.org/10.3213/1612-1651-10087

Friedman, I., Smith, R.L. (1960) A new dating method using obsidian: Part I, The development of the method. *American Antiquity*, Vol. 25, 476–493. https://doi.org/10.2307/276634

Friedman, I., Smith, R.L., Clark, D. (1963) Obsidian Dating. In: Brothwell, D., Higgs, E. (Eds.), Science in Archaeology, Thames and Hudson, London, pp. 47–58.

Glascock, M.D. (2002) Obsidian Provenance Research in the Americas. *Acc. Chem. Res.*, Vol. 35, 611–617. https://doi.org/10.1021/ar010041f

Glascock, M.D., Speakman, R.J., Popelka-Filcoff, R.S. (Eds.) (2007) *Archaeological Chemistry: Analytical Techniques and Archaeological Interpretation*. ACS Symposium Series, American Chemical Society, Washington, DC. https://doi.org/10.1021/bk-2007-0968

Halford, F.K., Haverstock, G.J., Rogers, A.K., Rosenthal, J.S., Skinner, C.E. (2008) *The Coleville and Bodie Hills NRCS Soil Inventory, Walker and Bridgeport, California: A Reevaluation of the Bodie Hills Obsidian Source (CA-MNO-4527) and its Spatial and Chronological Use*. Cultural Resources Report, U.S. Department of Interior, Bureau of Land Management, Bishop Field Office, Bishop, California.

Holm, R.J., Heilbronn, K., Saroa, D., Maim, G. (2023) Provenance of the Papuan Peninsula (Papua New Guinea): Zircon Inheritance from Miocene–Pliocene Volcanics and Volcaniclastics. *Geosciences*, Vol. 13, 324. https://doi.org/10.3390/geosciences13110324

John, D. A., du Bray, E.A., Blakely, R.J., Fleck, R.J., Vikre, P.G., Box, S.E., Moring, B.C. (2012) Miocene Magmatism in the Bodie Hills Volcanic Field, California and Nevada: A Long-lived Eruptive Center in the Southern Segment of the Ancestral Cascades Arc. *Geosphere* 8, 1, 44–97.

John, D.A., du Bray, E.A., Box, S.E., Vikre, P.G., Rytuba, J.J., Fleck, R.J., Moring, B.C. (2015) *Geologic map of the Bodie Hills, California and Nevada*. U.S. Geological Survey Scientific Investigations Map.

Karato, S. (2013) Rheological Properties of Minerals and Rocks. In: Karato, S. (Ed.*), Physics and Chemistry of the Deep Earth,* Wiley, pp. 94–144. https://doi.org/10.1002/9781118529492.ch4

Laskaris, N., and Liritzis, I. (2020) Surface and interface investigation of archaeological obsidian artefacts with TOF-SIMS: Case study. *Scientific Culture*, Vol. 6, No. 3, 85-99. https://doi.org/10.5281/ZENODO.4007733.

Lee, H.-H., Papaioannou, A., Novikov, D.S., Fieremans, E. (2020) In vivo observation and biophysical interpretation of time-dependent diffusion in human cortical gray matter. *NeuroImage*, Vol. 222, 117054. https://doi.org/10.1016/j.neuroimage.2020.117054.

Liritzis, I & Laskaris, N (2011) Fifty years of obsidian hydration dating in archaeology, *J. Non Crystalline Solids*, 357, 211-219.

Liritzis, I & Laskaris, N (2012) The SIMS-SS obsidian hydration dating Method. In I.Liritzis and C.M. Stevenson (Editors). *The Dating and Provenance of Natural and Manufactured Glasses*; (The University of New Mexico Press), 26-45.

Liritzis, I. (2014) Obsidian Hydration Dating. In: Rink, W.J., Thompson, J. (Eds.), *Encyclopedia of Scientific Dating Methods,* Springer Netherlands, Dordrecht, pp. 1–23. https://doi.org/10.1007/978-94-007-6326-5_39-1

Liritzis, I. (2006) SIMS-SS A new obsidian hydration dating method: Analysis and theoretical principles. *Archaeometry*, Vol. 48, 533–547. https://doi.org/10.1111/j.1475-4754.2006.00271.x

Liritzis, I., Andonache, I. (2024a) A first use of the power law and growth rate of experimentally aged obsidian hydration for dating purposes: Part I. *Scientific Culture*, Vol. 10, No 3, 101-134.

Liritzis, I., Andronache, I., Stevenson, C. (2024b) A novel approach to documenting water diffusion in ancient obsidian artifacts via the complexity analysis of microscope images. *Journal of Archaeological Science,* Vol. 161, 105896. https://doi.org/10.1016/j.jas.2023.105896

Liritzis, I and Andronache, I. (2024c) Further investigation of calibration for obsidian hydration dating using aged high temperature and long-term low temperature hydrated samples (submitted to JAS).

Liritzis, I., Diakostamatiou, M. (2002) Towards a new method of obsidian hydration dating with secondary ion mass spectrometry via a surface saturation layer approach. *Mediterranean Archaeology & Archaeometry*, Vol. 2, 3–20.

Liritzis, I., Diakostamatiou, M., Stevenson, C.M., Novak, S.W., Abdelrehim, I. (2004) Dating of hydrated obsidian surfaces by SIMS-SS. *Journal of Radioanalytical and Nuclear Chemistry*, Vol. 261, 51–60. https://doi.org/10.1023/B:JRNC.0000030934.66579.54

Liritzis, I., and Laskaris, N. (2021) Archaeological obsidian hydration dating with secondary ion mass spectrometry: Current status. *SCIENTIFIC CULTURE*, Vol. 21, No 3, pp. 51-67. https://doi.org/10.5281/ZENODO.5598229

Ma, D., Stoica, A.D., Wang, X.-L. (2009) Power-law scaling and fractal nature of medium-range order in metallic glasses. *Nature Materials*, Vol. 8, 30–34. https://doi.org/10.1038/nmat2340

Mazer, J.J., Stevenson, C.M., Ebert, W.L., Bates, J.K. (1991) The Experimental Hydration of Obsidian as a Function of Relative Humidity and Temperature. *American Antiquity*, Vol. 56, 504–513. https://doi.org/10.2307/280898.

McAlpine, J.R., Keig, G and Falls, R (1983) Climate of Papua New Guinea, Climate of Papua New Guinea. *Commonwealth Scientific and Industrial Research Organization in association with Australian National University Press,* Canberra, Australia.

Mitchell, P.A. (1989) *Geology, hydrothermal alteration and geochemistry of the Lamalele (D'Entrecasteaux Islands, Papua New Guinea) and Wairakei (North Island, New Zealand) geothermal areas*. PhD Thesis, University of Canterbury, Australia.

Moore, P. (2011) Obsidian sources of the Coromandel Volcanic Zone, Northern New Zealand. *Journal of the Royal Society of New Zealand*, *43*(1), 38–57. https://doi.org/10.1080/03036758.2011.576684.

Moore, P.R. (2012) Obsidian sources of the Taupo volcanic zone, central north island, New Zealand. *Rapa Nui Journal*, 26(2), 17-28.

Nakazawa, Y. (2016) The significance of obsidian hydration dating in assessing the integrity of Holocene midden, Hokkaido, northern Japan. *Quaternary International*, Vol. 397, 474–483. https://doi.org/10.1016/j.quaint.2015.01.029

Nakazawa, Y., Maeso, C.V., Carmona-Ballestero, E., Rissetto, J., Ordaz, A.B., Naoe, Y., Dohi, K., Araya, M., Nomura, H., Sumita, M., Schmincke, H.-U. (2023) Obsidian hydration dating helps understand prehispanic land use on the volcanic island of Tenerife, Canary Islands, Spain. *Quaternary International.* https://doi.org/10.1016/j.quaint.2023.08.009

Novak, S.W., Stevenson, C.M. (2012) Aspects of secondary ion mass spectrometry (SIMS) depth profiling for obsidian hydration dating. In: Liritzis, I., Stevenson, C.M. (Eds.), *Obsidian and Ancient Manufactured Glasses*, University of New Mexico Press, Albuquerque, pp. 15–25.

Novikov, D.S., Jensen, J.H., Helpern, J.A., Fieremans, E. (2014) Revealing mesoscopic structural universality with diffusion. *Proceedings of the National Academy of Sciences* USA, Vol. 111, 5088–5093. https://doi.org/10.1073/pnas.1316944111.

Rogers, A.K. (2007) Effective hydration temperature of obsidian: a diffusion theory analysis of time-dependent hydration rates. *Journal of Archaeological Science*, Vol. 34, 656–665. https://doi.org/10.1016/j.jas.2006.07.005

Rogers, A. K. (2008a) Field data validation of an algorithm for computing obsidian effective hydration temperature. *Journal of Archaeological Science*, Vol. 35, 441–447. https://doi.org/10.1016/j.jas.2007.04.009

Rogers, A. K. (2008b) Obsidian hydration dating: accuracy and resolution limitations imposed by intrinsic water variability. *Journal of Archaeological Science*, Vol. 35, 2009–2016. https://doi.org/10.1016/j.jas.2008.01.006

Rogers, A. (2012) Temperature correction for obsidian hydration dating. In: Obsidian and Ancient Manufactured Glasses, pp. 46–55.

Rogers, A., Yohe, R. (2011) An improved equation for Coso obsidian hydration dating, based on obsidian-radiocarbon association. *Society of California Archaeology Proceedings*, Vol. 25, 1-15.

Rogers, A.K., Duke, D. (2011) An archaeologically validated protocol for computing obsidian hydration rates from laboratory data. *Journal of Archaeological Science*, Vol. 38, 1340–1345. https://doi.org/10.1016/j.jas.2011.01.012

Rogers, A.K., Stevenson, C.M., (2022a) An equation relating obsidian hydration rate to temperature and structural water content. *IAOS Bulletin* 1–15.

Rogers, A.K and Stevenson, C.M. (2022b) A summary of obsidian hydration dating science and method for archaeologists. *Working Paper MS234A*.

Rogers, A., Stevenson, C.M. (2023) An Accuracy Study of Obsidian Hydration Dating Based upon Radiocarbon Pairing. https://doi.org/10.2139/ssrn.4522888

Rogers, A.K., Stevenson, C.M. (2023) Obsidian Hydration Dating: Summary and Status of a Physics-Based Approach. *California Archaeology*, Vol. 15, 219–242. https://doi.org/10.1080/1947461X.2023.2240124

Singer, R., Wymer, J. (1982) *The Middle Stone Age at Klasies River Mouth in South Africa* (Doctoral Dissertation). Stellenbosch University, Stellenbosch.

Smith, C.I., Chamberlain, A.T., Riley, M.S., Stringer, C., Collins, M.J. (2003) The thermal history of human fossils and the likelihood of successful DNA amplification. *Journal of Human Evolution*, Vol. 45, 203–217. https://doi.org/10.1016/S0047-2484(03)00106-4.

Stevenson, C.M. (1993) Archaeological Investigations at an Island Rectangular House (Site 10-244), Easter Island. *Rapa Nui Journal*, Vol. 7, 25–27, 38–44.

Stevenson, C., Liritzis, I., Diakostamatiou, M. (2002) Investigations towards the hydration dating of Aegean obsidian. *Mediterranean Archaeology & Archaeometry*, Vol. 2, 93–109.

Stevenson, C.M., Novak, S.W. (2011) Obsidian hydration dating by infrared spectroscopy: method and calibration. *Journal of Archaeological Science*, Vol. 38, 1716–1726. https://doi.org/10.1016/j.jas.2011.03.003

Stevenson, C.M., Rogers, A.K., Glascock, M.D. (2019a) Variability in obsidian structural water content and its importance in the hydration dating of cultural artifacts. *Journal of Archaeological Science: Reports*, Vol. 23, 231–242. https://doi.org/10.1016/j.jasrep.2018.10.032.

Stevenson, C.M., Williams, C., Carpenter, E., Hunt, C.S., Novak, S.W. (2019b) Architecturally Modified Caves on Rapa Nui: Post-European Contact Ritual Spaces? *Rapa Nui Journal*, Vol. 32, 1–36. https://doi.org/10.1353/rnj.2019.0005.

Stevenson, C.M., Rogers, A.K., Haverstock, G. (2021) A Brief Note on Hydration Rates for the Bodie Hills Obsidian Regional Source, Eastern California, Based on Infrared Spectroscopy and Optical Measurement. *International Association for Obsidian Studies Bulletin,* Vol. 67, 30–35.

Stevenson, C.M., Rogers, A.K., Novak, S.W., Ambrose, W., Ladefoged, T.N. (2021) A molecular model for obsidian hydration dating. *Journal of Archaeological Science: Reports*, Vol. 36, 102824. https://doi.org/10.1016/j.jasrep.2021.102824.

Stevenson, C.M., Rogers, A.K., Haverstock, G. (2024) Hydration rates for Bodie Hills obsidian regional source, based upon infrared spectroscopy and optical measurement. In: Bourdonnec, F.-X.L., Orange, M., Shackley, M.S. (Eds.), *Sourcing Obsidian - A State-of-the-Art in the Framework of Archaeological Research.* Springer Nature, Switzerland.

Tostanoski, N.J., Sundaram, S.K. (2023) Universal power-law of terahertz optical properties of borosilicate, tellurite, and chalcogenide glass families. *Scientific Reports*, Vol. 13, 2260. https://doi.org/10.1038/s41598-023-29345-x

Von Aulock, F.W., Kennedy, B.M., Schipper, C.I., Castro, J.M., Martin, D.E., Oze, C., Watkins, J.M., Wallace, P.J., Puskar, L., Bégué, F., Nichols, A.R.L., Tuffen, H. (2014) Advances in Fourier transform infrared spectroscopy of natural glasses: From sample preparation to data analysis. *Lithos,* Vol. 206–207, 52–64. https://doi.org/10.1016/j.lithos.2014.07.017.

Webb, S.L. (2021) Thermal stress, cooling-rate and fictive temperature of silicate melts. *Contributions to Mineralogy and Petrology*, Vol. 176, 78. https://doi.org/10.1007/s00410-021-01836-y

Zeng, Q., Lin, Y., Liu, Y., Zeng, Z., Shi, C.Y., Zhang, B., Lou, H., Sinogeikin, S.V., Kono, Y., Kenney-Benson, C., Park, C., Yang, W., Wang, W., Sheng, H., Mao, H., Mao, W.L. (2016) General 2.5 power law of metallic glasses. *Proceedings of the National Academy of Sciences* USA, Vol. 113, 1714–1718. https://doi.org/10.1073/pnas.1525390113

Zhang, Y., Behrens, H. (2000) H2O diffusion in rhyolitic melts and glasses. *Chemical Geology*, Vol. 169, 243–262. https://doi.org/10.1016/S0009-2541(99)00231-4

Zhang, Y., Stolper, E.M., Wasserburg, G.J. (1991) Diffusion of water in rhyolitic glasses. *Geochimica et Cosmochimica Acta*, Vol. 55, 441–456. https://doi.org/10.1016/0016-7037(91)90003-N

***

APPENDIX

Table A1 (A, B, C, D). (A) Wekwok source, Wekwok Lou island, Papua, New Guinea. The four low T aged data; Full width half maximum and sloping or end point, (B) Umleang source on Lou Island in the Manus Group of Papua New Guinea, both 0.10% OH (Ambrose et al., 2004a, b; Novak & Stevenson, 2012), c) The high T experimental data at 140-180 °C. NB: Low water content 0.10%: BH1, Wekwok, Umleang, Peru. High Water content 0.21-0.25%: BH2, NZ, Mexico. RBC=Richard Bland College lab number.

(A)

WEKWOK, T°C	Duration, years	FWHM depth, um	End Point, um
10	15.2	0.204	0.377
20	15.6	0.386	0.479
30	15.6	0.650	0.902
40	11.6	0.905	1.360

(B)

UMLEANG, T°C	Duration, years	FWHM depth, um	End point
10	26.2	0.200	0.308
20	26.2	0.279	0.378
30	26.2	0.667	0.745
40	26.2	1.150	1.458

(C)

		Obsid-ian		Hydra-tion time	Optical 200x	Pixels/Year	
	Lab No.	**Source**	**Tempera-ture ^{o}C**	**Days**	**Rim Width (um)**		
						X20	X60
Mex-ico	RBC-838	UC-16A	180	50	18,0	1688213 (x20)	5973035
	RBC-839	UC-16A	170	50	14,1	2750239	8119885
	RBC-840	UC-16A	160	50	11,4	3810505	11120784
	RBC-841	UC-16A	150	50	9,0	4757629	15299209
	RBC-842	UC-16A	140	50	6,6	5816399	21021744
Peru	RBC-796	CPQ009F	180	30	15,5	2407248	7224876
	RBC-797	CPQ009F	170	30	12,9	3654477	10679194
	RBC-798	CPQ009F	160	30	10,2	4950264	14828028
	RBC-799	CPQ009F	150	30	8,4	6125114	19437503
	RBC-807	CPQ009F	140	30	6,0	7308541	25083992
NZ, x60	RBC-849	Hahei, NZ	180	32	10,8	3730859	3730858
	RBC-850	Hahei, NZ	170	46	10,5	5101039	4345329
	RBC-851	Hahei, NZ	160	55	9,6	7099091	4820370
	RBC-852	Hahei, NZ	150	69	7,5	9306508	5285177
	RBC-853	Hahei, NZ	140	81	6,6	16355650	6461491
BH2	RBC-724	SA 4D	140	60	7,0		
	RBC-725	SA 4D	150	60	9,2		
	RBC-726	SA 4D	160	60	11,9		
	RBC-727	SA 4D	170	60	15,2		
	RBC-728	SA 4D	180	60	18,9		
BH1	RBC-719	SA 13J	140	60	7,9	555108	
	RBC-720	SA 13J	150	60	9,9	589980	
	RBC-721	SA 13J	160	60	12,5	661254	
	RBC-722	SA 13J	170	60	16,1	1019712	
	RBC-723	SA 13J	180	60	19,9	1163196	

Various Power Law plots

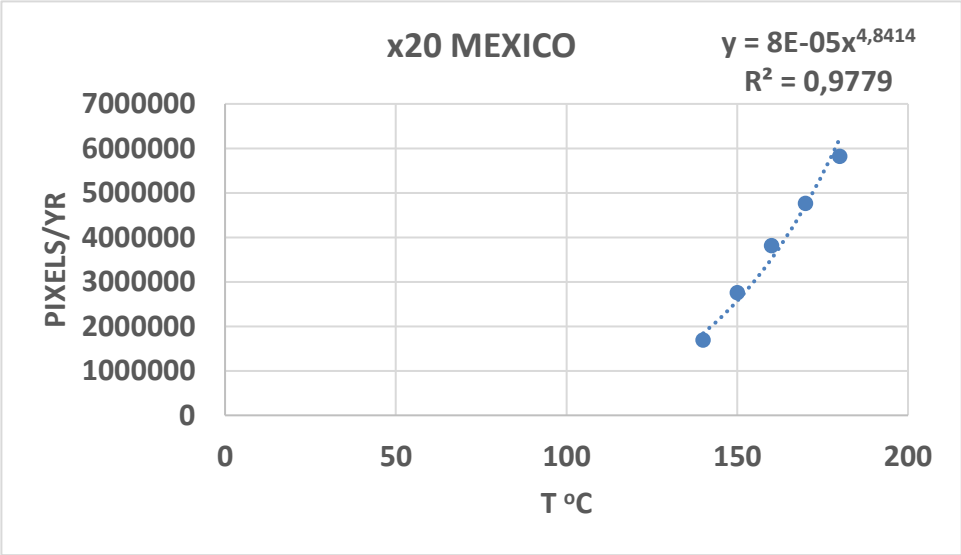

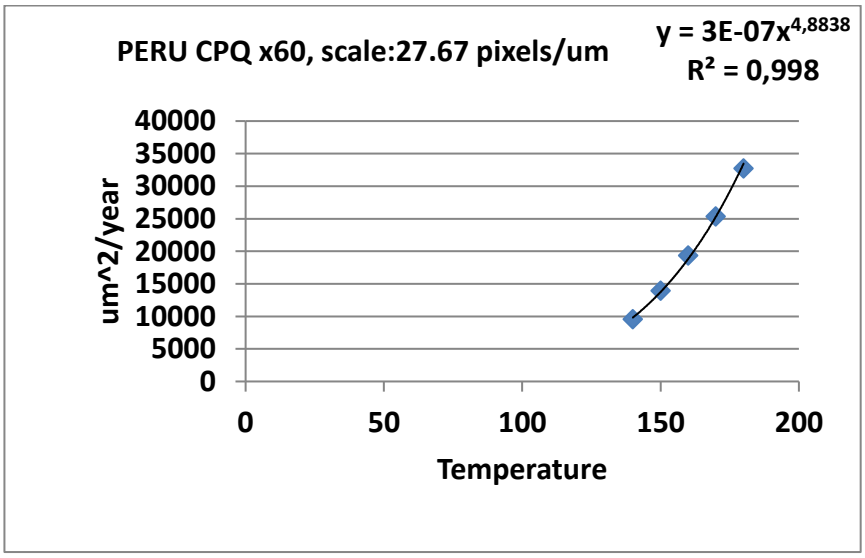

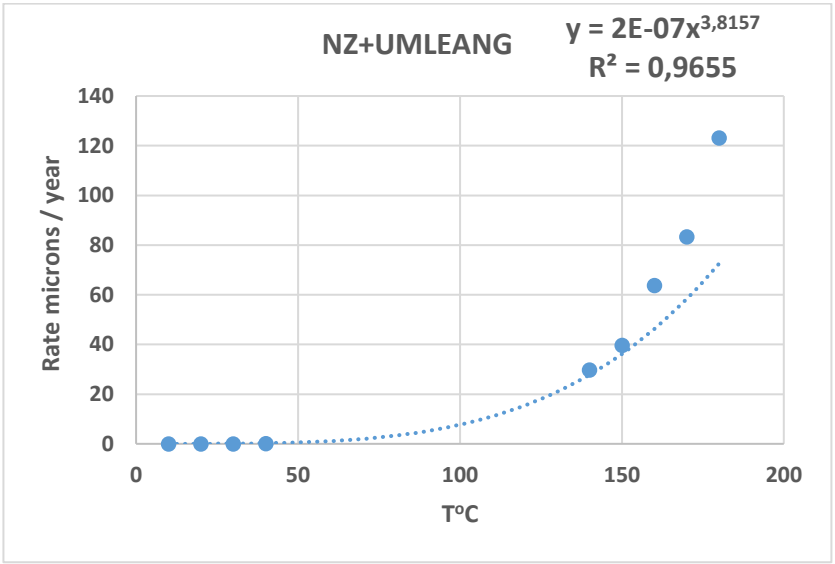

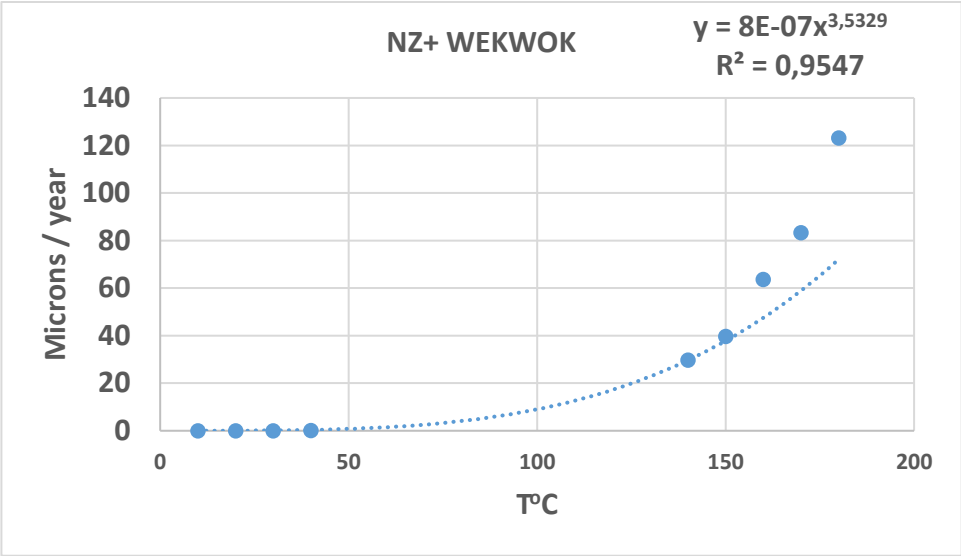
NZ+ WEKWOK
y = 8E-07x^3,5329
R² = 0,9547
Microns / year
TºC
0
20
40
60
80
100
120
140
0
50
100
150
200

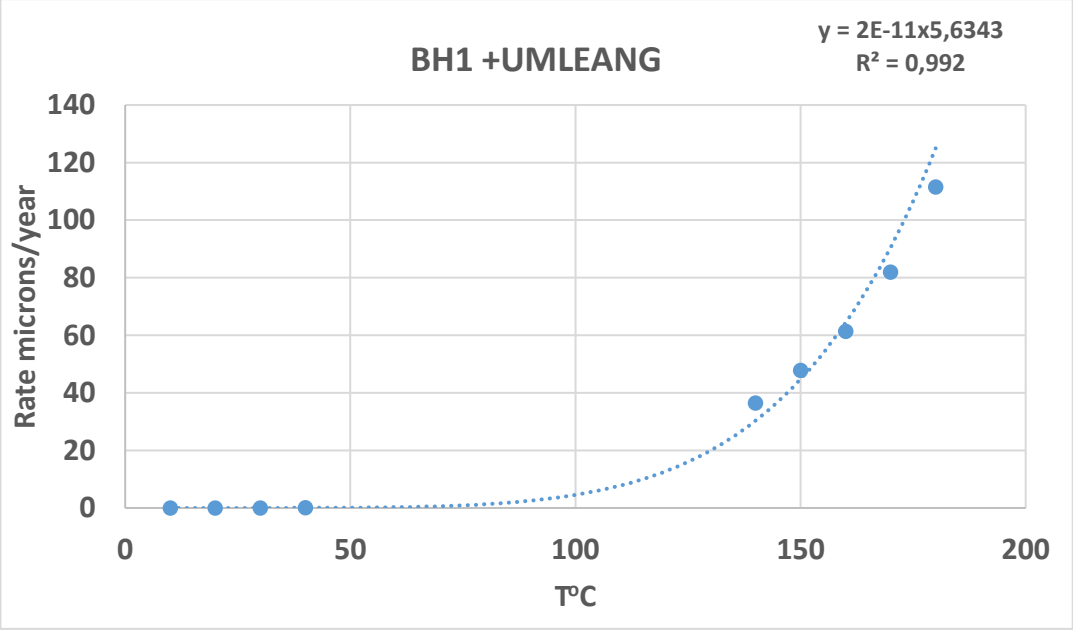
BH1 +UMLEANG
y = 2E-11x5,6343
R² = 0,992
Rate microns/year
TºC
0
20
40
60
80
100
120
140
0
50
100
150
200

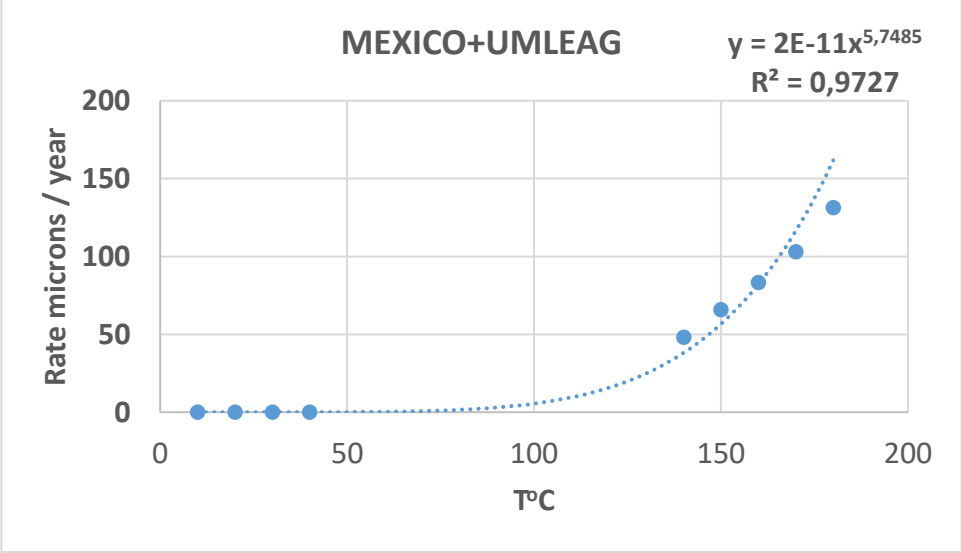
MEXICO+UMLEAG
y = 2E-11x^5,7485
R² = 0,9727
Rate microns / year
TºC
0
50
100
150
200
0
50
100
150
200

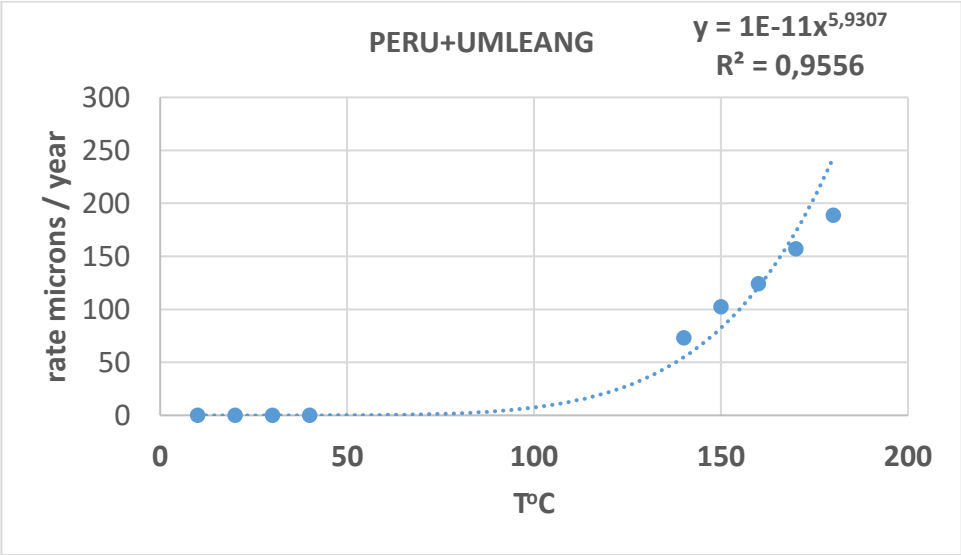

Figure A1: Various Power law plots

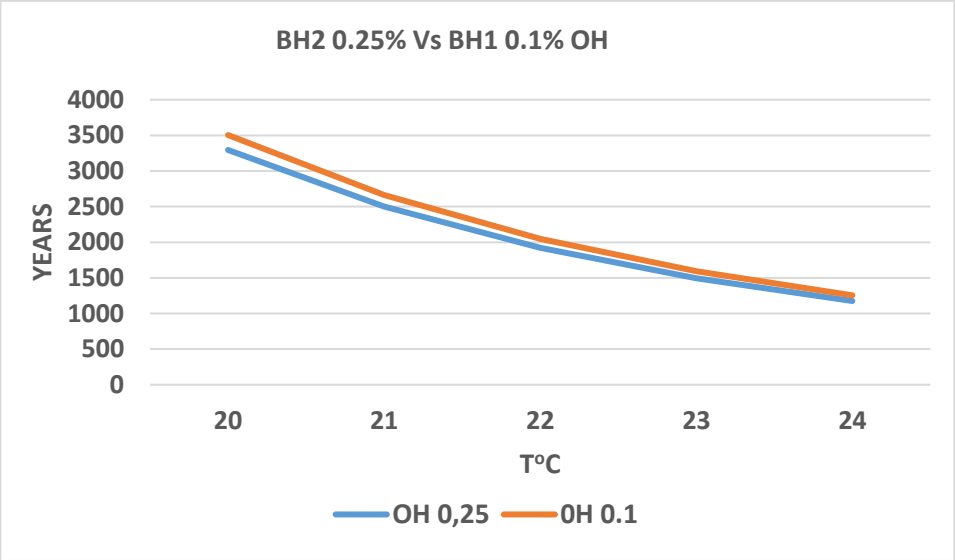

Figure A2: Age Difference for same T and different OH% of BH1+Umleang and BH2+Umleang. For higher than 23-24ºC the ages overlap.

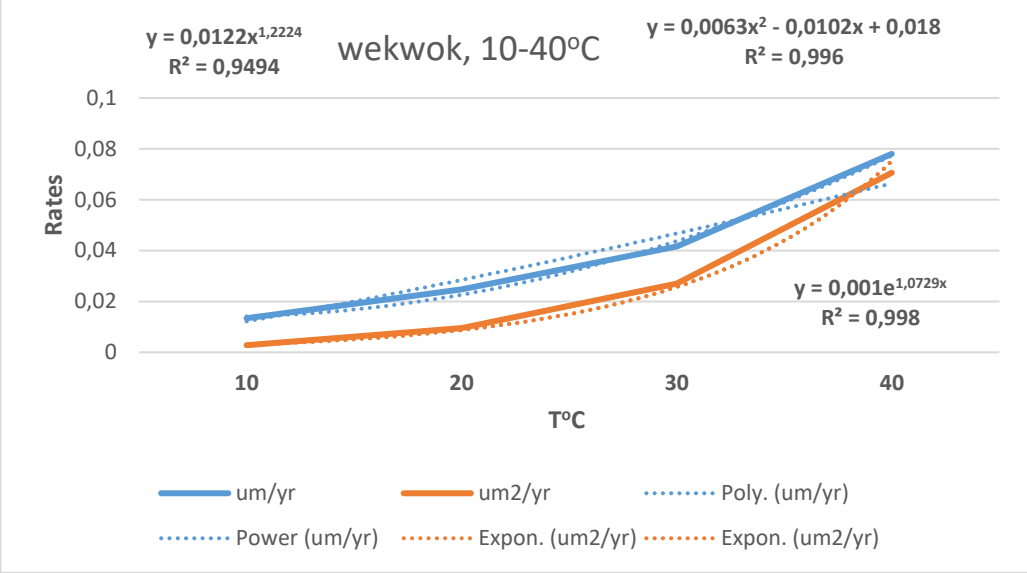

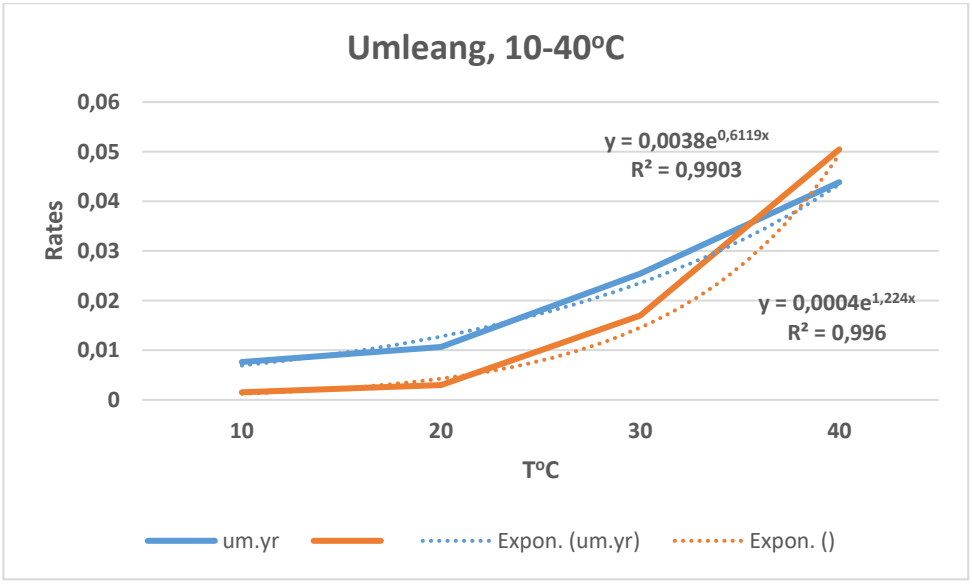

Figure A3: Rates as um/year and um²/year for the two sources from New Guinea and low T aged laboratory induced hydration data.